NUMERICAL INTEGRATION OF A NINE-LEVEL GLOBAL PRIMITIVE EQUATIONS MODEL FORMULATED BY THE BOX METHOD

YOSHIO KURIHARA[1]

Meteorological Research Institute, Suginami, Tokyo, Japan

and

J. LEITH HOLLOWAY, JR.

Geophysical Fluid Dynamics Laboratory, ESSA, Washington, D.C.

ABSTRACT

Based on the box method, finite-difference versions of a system of primitive equations in spherical coordinates are formulated for a spherical grid. Non-linear computational instability cannot occur in time integrations of these equations. Conservation of total mass is guaranteed by the finite-difference form of the continuity equation. The proposed scheme yields no fictitious sources of energy in the derivation of the difference formula for the budget of the total energy over the entire domain. The finite-difference equations for the budget of the relative and absolute angular momentum are not exact analogs of the continuous forms but nevertheless are very accurate.

This system of primitive equations for a nine-level general circulation model of the atmosphere has been numerically integrated for 50 forecast days. The network of grid points covers the entire globe with nearly uniform spacing and has no artificial horizontal boundaries. The initial data were latitude-height-dependent zonal mean winds and pressures and zonal mean temperatures perturbed slightly by random numbers. The time integration was carried out without any finite-difference computational problems and baroclinic waves developed and propagated.

LIST OF SYMBOLS

a	mean radius of earth
A_l	lateral interface between box 0 and box l
$A, B, \ldots Z$	scalar variable or vector component
C_D	drag coefficient
c_p	specific heat at constant pressure
c_v	specific heat at constant volume
$\mathcal{D}_2, \mathcal{D}_3$	two- and three-dimensional divergence operators (see section 2)
$D(\mathcal{Y})$	D operator (see section 2)
D_T	tension rate of strain
D_S	shearing rate of strain
$\|D\|$	pure deformation
(DIS)	internal dissipation of kinetic energy
$E_\lambda(AB)$	E operator (see section 2)
f	Coriolis parameter
F	source term for X.
F_λ, F_θ	frictional forces in zonal and meridional directions
F_T	effect of thermal diffusion
g	acceleration of gravity
$G_\lambda(A), G_\theta(A)$	G operators (see section 2)
$H_1(\mathcal{Y}), H_2(Y)$	H operators (see section 2)
k	level number
k_0	non-dimensional parameter in non-linear horizontal viscosity
K	number of layers in the model
K_H	horizontal eddy viscosity coefficient
K_V	vertical eddy viscosity coefficient
$L_\lambda(A, B), L_\theta(A, B)$	L operators (see section 2)
$\hat{m}$	coefficient in metric term of equation of motion
$M(\mathcal{Y})$	M operator (see section 2)
$N_1(\mathcal{Y}), N_2(Y)$	N operators (see section 2)
$\dot{q}$	heat added per unit mass
P	pressure
P_*	surface pressure
R	gas constant for dry air
S	surface of a box
ΔS	horizontal area of a box
t	time
T	temperature
u	eastward component of wind
U, V	wind components at poles
v	northward component of wind
v_n	outward component of wind velocity on surface of box
$\mathbf{V}$	three-dimensional velocity vector
$\mathbf{V}_H$	horizontal velocity vector
$V, \Delta V$	volume of a box
w	weight$=A_l/\Delta V$
(WKLT)	work done by wind stress through lateral boundaries
(WKSG)	work done by wind stress through sigma surfaces

[1] Present affiliation: Geophysical Fluid Dynamics Laboratory, ESSA, Washington, D.C.

X	a scalar; a component of Reynolds stress tensor
$\overline{X}$	mean value of X
Y	a function of $A, B, \ldots Z$ or a constant
$\mathcal{Y}$	a function of Y_0 and Y_1 or a constant
z_*	height of ground surface
$\nabla\cdot$	three-dimensional divergence operator
$\nabla_H\cdot$	horizontal divergence operator
α	$a \cos\theta$
γ	diffusive flux of heat
Γ	ratio of pure deformation to square of wave number
$\Delta\theta$	latitude increment
$\Delta\lambda$	longitude increment
$\delta\sigma$, $\Delta\sigma$	sigma increment
θ	latitude
κ_{eff}	effective wave number
λ	longitude
ρ	density
σ	vertical coordinate$=P/P_*$
τ	stress
ϕ	geopotential of sigma surface
ω	vertical P-velocity
$\dot{\sigma}$	vertical σ-velocity
Ω	angular velocity of earth's rotation

1. INTRODUCTION

In this study, spherical coordinates are used rather than a map coordinate system and thus map projection factors do not appear in the equations. Furthermore, we have used a network of grid points nearly uniformly spaced over the entire globe. The analysis of a time integration of a general circulation model is facilitated when use is made of a coordinate system and grid network more naturally suited to a global problem.

Previous to this study, Kurihara [2] carried out test computations on a barotropic primitive equation model on the special grid network which we have adopted in this research. His tests were successful, but his computation scheme, involving a number of interpolations, was complicated. In this study this complication has been avoided by means of the box method.

It has been known for some time that for the purpose of deriving the finite-difference form of the differential equations for an arbitrarily chosen grid or general polygonal mesh, there is a method which preserves the conservation properties of the original differential equations and at the same time yields an empirically accurate difference approximation [5, 6]. In addition, Bryan [1] recently proved that the method can also satisfy a quadratic-conserving condition by means of a special form to approximate the divergence of a quantity. We apply this method, which we shall call the "box method" to a system of primitive equations in spherical coordinates to formulate the energy-conserving finite-difference forms.

The principle of the box method is simple. Imagine a space domain containing volume elements of different sizes. Consider the equation:

$$\frac{\partial X}{\partial t}=-\nabla\cdot(\mathbf{V}X)+F \tag{1.1}$$

where X is a scalar quantity; $\mathbf{V}$, a three-dimensional velocity vector; $\nabla\cdot$, a three-dimensional divergence operator; and F is a source term of the quantity X. Integration of the equation (1.1) over a volume element or a "box" gives

$$\frac{\partial \overline{X}}{\partial t}=-\frac{1}{V}\oint v_n X dS+\frac{1}{V}\int F dV \tag{1.2}$$

In (1.2), $\overline{X}$ denotes a mean value of X for a box of volume V and surface area S. The Gauss theorem is applied in deriving the first term on the right-hand side, where v_n is the outward component of velocity on the box surface. The second term represents the mean effect of a source or external force. The approximation of the first term by the box method is made by estimating the flow of a quantity to or from all the adjacent boxes. Notice that if the boxes are regularly placed, the box method takes a form similar to the energy-conserving scheme proposed by Lilly (see the Appendix of [4]) and adopted by Smagorinsky, Manabe, and Holloway [4].

In this formulation, it is desirable that the corresponding finite-difference scheme does not create in the mean a fictitious source for the quantity X or its variance. Bryan [1] has shown how to establish the schemes which satisfy the above requirement and, therefore, are free from the so-called non-linear computational instability. The requirement for the finite-difference form of the source term, i.e., the second term on the right-hand side of equation (1.2), is that, if it contains any transformations from another quantity, numerical consistency should exist. For example, in a system of energy equations which are derived from the finite-difference expressions of the primitive equations, the conversion between the two different types of energy must appear in the two corresponding equations as the same expression but of opposite sign.

The formulation of the computation schemes for the system of primitive equations satisfying the above requirements is presented in section 3. In section 4 the energy consistency of the proposed schemes is discussed, and in section 5 the results of a numerical integration of the system of equations for a global nine-level model is presented.[2]

2. FINITE-DIFFERENCE OPERATORS AND THEIR CHARACTERISTICS

In this section, we shall present definitions of some of the finite-difference operators. Since the box method will be

[2] During the preparation of this paper, we learned of work by M. Grimmer and D. B. Shaw of the British Meteorological Office, who derived a finite-difference formulation of the equations for a barotropic model in a manner similar to ours. The results of their investigation are to be published.

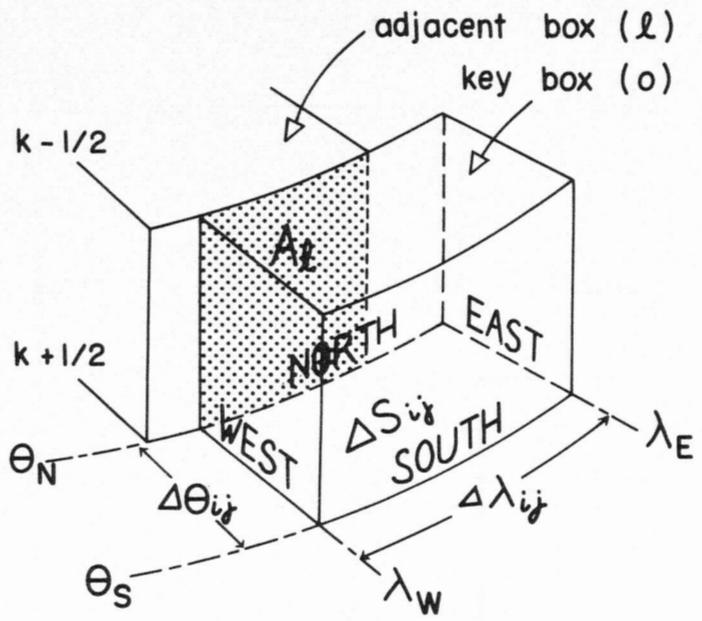

FIGURE 1.—Pictorial view of a key box (0) at latitude θ_{ij} and longitude λ_{ij} and part of an adjacent box (l) to the north. The two boxes touch each other along area A_l at latitude $\theta_N=\theta_{ij}+\Delta\theta_{ij}/2$.

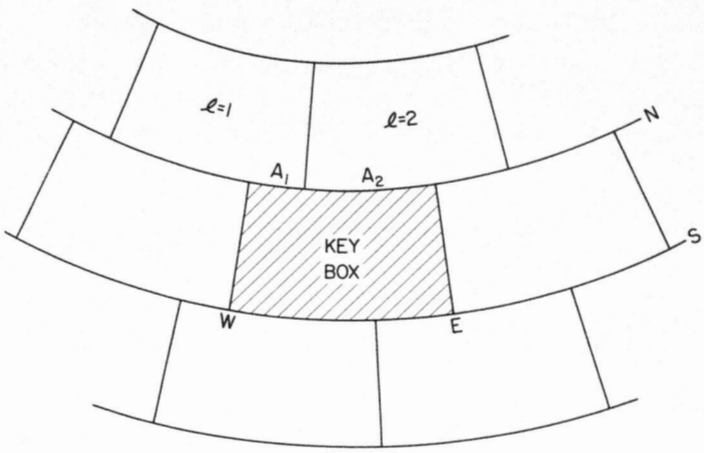

FIGURE 2.—Diagram of a key box surrounded by six adjacent boxes. On the north the key box joins box one at interface A_1, and box two at interface A_2. Two additional boxes, of course, contact the key box on the top and bottom.

applied later to the equations written in the so-called σ-coordinate system on the sphere, it is convenient to define a volume element as being bounded by two constant latitude surfaces, two constant longitude surfaces, and two constant sigma surfaces, as shown in figure 1. We consider that a key box has the indices (i, j, k) corresponding to the λ, θ, and σ coordinates. The center of the box is located at latitude θ_{ij}, longitude λ_{ij} and $\sigma=\sigma_k$. Then the latitudes and longitudes of the lateral sides of the box are represented by $\theta_N=\theta_{ij}+(\Delta\theta_{ij}/2)$, $\theta_S=\theta_{ij}-(\Delta\theta_{ij}/2)$, $\lambda_E=\lambda_{ij}+(\Delta\lambda_{ij}/2)$, and $\lambda_W=\lambda_{ij}-(\Delta\lambda_{ij}/2)$. The upper and the lower surfaces are given by $\sigma=\sigma_{k-1/2}$ and $\sigma=\sigma_{k+1/2}$, respectively. We assume that the boxes are connected in the vertical direction to form columns and that the sigma levels are common to all columns.

Hereafter, the value of X in a key box will be denoted by X_{ijk} or X_0 or X_{0k}, and that of an adjacent box by X_l.

The horizontal cross-section and the volume of a box shown in figure 1 are given by (2.1) and (2.2), respectively.

$$\Delta S_{ij}=2a^2\sin\left(\frac{\Delta\theta_{ij}}{2}\right)\cos\theta_{ij}\Delta\lambda_{ij} \tag{2.1}$$

$$\Delta V_{ijk}=\Delta S_{ij}(\sigma_{k+1/2}-\sigma_{k-1/2}) \tag{2.2}$$

Letting A_l=the area of a lateral interface between the key box and a contiguous box l, we define a weight w_l,

$$w_l=A_l/\Delta V_{ijk} \tag{2.3}$$

which has the dimension of (length)$^{-1}$. In the particular case of our spherical grid system, the number of interfaces at the east and west sides is just one as seen in figure 2. However, we shall assume here that there is more than one interface even at these sides for the sake of generality. Taking the symbols $\sum_E$, $\sum_W$, $\sum_N$, and $\sum_S$ for the summation with respect to the interfaces at the east, west, north, and south sides of the box, respectively, we have

$$w_E=w_W \quad \text{but} \quad w_N\neq w_S$$

where $w_E=\sum_E w_l$, $w_W=\sum_W w_l$, $w_N=\sum_N w_l$, and $w_S=\sum_S w_l$.

In defining the finite-difference operators we employ the following notations:

u=eastward wind velocity
v=northward wind velocity
$\bar{\omega}$=vertical σ-velocity$=d\sigma/dt$
P_*=surface pressure$\equiv$pressure at $\sigma=1$
$A, B, \ldots, Z$=scalar variable or vector component
Y=function of $A, B, \ldots, Z$ or constant
$\mathcal{Y}$=a quantity which is defined as a function of Y_0 and Y_l, or a constant
a=mean radius of the earth
$\alpha=a\cos\theta$
$dS=a^2\cos\theta\, d\lambda d\theta$
$dV=a^2\cos\theta\, d\lambda d\theta d\sigma$

$\mathcal{D}_2(\ )$=two-dimensional divergence operator

$$=\frac{\partial(\ )P_*u}{a\cos\theta\partial\lambda}+\frac{\partial(\ )P_*v\cos\theta}{a\cos\theta\partial\theta}$$

$\mathcal{D}_3(\ )$=three-dimensional divergence operator

$$=\mathcal{D}_2(\ )+\frac{\partial(\ )P_*\bar{\omega}}{\partial\sigma}$$

Assume that u, v, and variables $A, B, \ldots, Z$ are given on the σ-levels of integer k's as shown in figure 3, and $\bar{\omega}$ is computed at the tops and bottoms of the boxes, i.e., on the integer levels plus or minus a half.

DEFINITION OF FINITE-DIFFERENCE OPERATORS

Assume that the expressions in continuous form on the left-hand sides of the formulas below are approximated by the corresponding finite-difference operators on the right-hand sides.

$$\frac{1}{\Delta V}\iiint_{\Delta V}\mathcal{D}_3(Y)dV \rightarrow D(\mathcal{Y}) \text{ or } M(\mathcal{Y})$$

$$\frac{1}{\Delta S}\iint_{\Delta S}\mathcal{D}_2(Y)dS \rightarrow H_1(\mathcal{Y}),\ H_2(Y),\ N_1(\mathcal{Y}) \text{ or } N_2(Y)$$

$$\frac{1}{\Delta V}\iiint_{\Delta V}\frac{\partial(AB\ldots Z)}{\alpha\partial\lambda}dV \rightarrow G_\lambda(AB\ldots Z)$$

$$\frac{1}{\Delta V}\iiint_{\Delta V}\frac{\partial(AB\ldots Z)}{a\partial\theta}dV \rightarrow G_\theta(AB\ldots Z)$$

$$\frac{1}{\Delta V}\iiint_{\Delta V}B\frac{\partial A}{\alpha\partial\lambda}dV \rightarrow L_\lambda(B,A)$$

$$\frac{1}{\Delta V}\iiint_{\Delta V}B\frac{\partial A}{a\partial\theta}dV \rightarrow L_\theta(B,A)$$

$$\frac{1}{\Delta V}\iiint_{\Delta V}\frac{\partial}{\partial\sigma}(AB\ldots Z)dV \rightarrow \frac{\delta_k(AB\ldots Z)}{\delta_k\sigma}$$

The functional forms of these operators follow. The notation $(\sum_N-\sum_S)$ and $(\sum_E-\sum_W)$ denote the difference between the sums of a quantity along the north and south sides and that between the sums along the east and west sides, respectively.

$$\left.\begin{aligned}
D(\mathcal{Y}) &= \left(\sum_E-\sum_W\right)\left\{\frac{u_l+u_0}{2}\frac{P_{*l}+P_{*0}}{2}\mathcal{Y}\,w_l\right\}\\
&\quad+\left(\sum_N-\sum_S\right)\left\{\frac{v_l+v_0}{2}\frac{P_{*l}+P_{*0}}{2}\mathcal{Y}\,w_l\right\}\\
&\quad+\frac{P_{*0}}{\sigma_{k+\frac12}-\sigma_{k-\frac12}}(\bar\omega_{0k+\frac12}\mathcal{Y}-\bar\omega_{0k-\frac12}\mathcal{Y})\\
M(\mathcal{Y}) &= \left(\sum_E-\sum_W\right)\left\{\frac{P_{*0}u_0+P_{*l}u_l}{2}\mathcal{Y}\,w_l\right\}\\
&\quad+\left(\sum_N-\sum_S\right)\left\{\frac{P_{*0}v_0+P_{*l}v_l}{2}\mathcal{Y}\,w_l\right\}\\
&\quad+\frac{P_{*0}}{\sigma_{k+\frac12}-\sigma_{k-\frac12}}(\bar\omega_{0k+\frac12}\mathcal{Y}-\bar\omega_{0k-\frac12}\mathcal{Y})
\end{aligned}\right\} \quad (2.4)$$

$$\left.\begin{aligned}
H_1(\mathcal{Y}) &= D(\mathcal{Y})-[\text{the last term of } D(\mathcal{Y})]\\
N_1(\mathcal{Y}) &= M(\mathcal{Y})-[\text{the last term of } M(\mathcal{Y})]
\end{aligned}\right\} \quad (2.5)$$

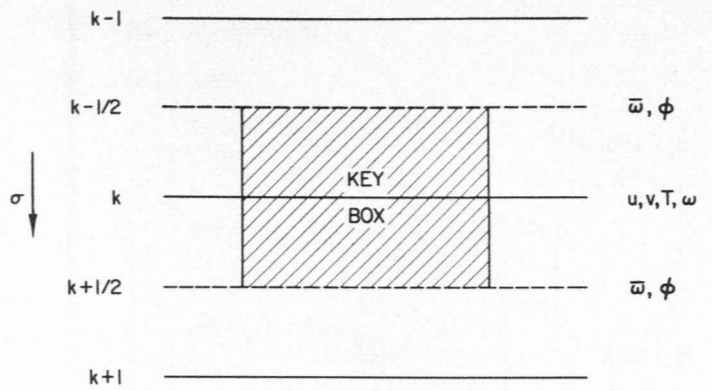

FIGURE 3.—Vertical cross-section of a key box showing that the variables u, v, T, and ω are defined at integer k levels whereas $\bar\omega$ and ϕ are defined at half-integer levels or at the horizontal interfaces at the top and bottom of the key box.

$$\left.\begin{aligned}
H_2(Y) &= \left(\sum_E-\sum_W\right)\left\{\frac{P_{*l}+P_{*0}}{2}\frac{Y_lu_0+Y_0u_l}{2}w_l\right\}\\
&\quad+\left(\sum_N-\sum_S\right)\left\{\frac{P_{*l}+P_{*0}}{2}\frac{Y_lv_0+Y_0v_l}{2}w_l\right\}\\
N_2(Y) &= \left(\sum_E-\sum_W\right)\left\{\frac{P_{*0}u_0Y_l+P_{*l}u_lY_0}{2}w_l\right\}\\
&\quad+\left(\sum_N-\sum_S\right)\left\{\frac{P_{*0}v_0Y_l+P_{*l}v_lY_0}{2}w_l\right\}
\end{aligned}\right\} \quad (2.6)$$

$$G_\lambda(AB\ldots Z)=\left(\sum_E-\sum_W\right)\left\{\frac{A_l+A_0}{2}\cdot\frac{B_l+B_0}{2}\cdots\frac{Z_l+Z_0}{2}w_l\right\} \quad (2.7)$$

$$G_\theta(AB\ldots Z)=\left(\sum_N-\sum_S\right)\left\{\frac{A_l+A_0}{2}\cdot\frac{B_l+B_0}{2}\cdots\frac{Z_l+Z_0}{2}w_l\right\}-(A_0B_0\ldots Z_0)(w_N-w_S) \quad (2.8)$$

$$L_\lambda(B,A)=\frac12\left[\sum_E\left\{\frac{B_l+B_0}{2}(A_l-A_0)w_l\right\}+\sum_W\left\{\frac{B_l+B_0}{2}(A_0-A_l)w_l\right\}\right] \quad (2.9)$$

$$L_\theta(B,A)=\frac12\left[\sum_N\left\{\frac{B_l+B_0}{2}(A_l-A_0)w_l\right\}+\sum_S\left\{\frac{B_l+B_0}{2}(A_0-A_l)w_l\right\}\right] \quad (2.10)$$

$$\frac{\delta_k(AB\ldots Z)}{\delta_k\sigma}=(A_{k+\frac12}B_{k+\frac12}\ldots Z_{k+\frac12}-A_{k-\frac12}B_{k-\frac12}\ldots Z_{k-\frac12})/(\sigma_{k+\frac12}-\sigma_{k-\frac12}) \quad (2.11)$$

Another operator required is

$$E_\lambda(AB)=\left(\sum_E-\sum_W\right)\left\{\frac{A_0B_l+A_lB_0}{2}w_l\right\}$$

This is a difference analog of the gradient of AB in the zonal direction. The quantity grid distance does not appear explicitly in the above formulas but rather quantities measuring the size of the box and the area of the interfaces.

The difference operators $D(\mathcal{Y})$ and $H_1(\mathcal{Y})$ differ from $M(\mathcal{Y})$ and $N_1(\mathcal{Y})$ in the manner of estimation of the transport of a given quantity. Note that the former schemes resemble the "filtered factor" form, after the terminology of Shuman [3]. However, the latter schemes resemble the "semi-momentum" form. For example, the quantity P_*u, which is the transport velocity of a property across the interface of two boxes 0 and l separated by a north-south boundary, is estimated in the former by

$$P_*u \rightarrow \frac{P_{*0}+P_{*l}}{2}\cdot\frac{u_0+u_l}{2}$$

whereas in the latter this term is computed by

$$P_*u \rightarrow \frac{P_{*0}u_0+P_{*l}u_l}{2}$$

Shuman [3] has shown that both forms are suitable for stable numerical integration of a system of non-linear equations which he derived. Furthermore, in either case, by approximating a transported quantity at the interfaces of two adjoining boxes by a mean value for the two boxes as suggested by Bryan [1], we are able to make the flux divergence term in any equation free from the so-called non-linear computational instability.

CHARACTERISTICS OF THE OPERATORS

The following are important characteristics of the operators.

(1) If a quantity $\mathcal{Y}$ is invariant with the exchange of the box indices 0 and l, e.g., $\mathcal{Y}=Y_0Y_l$ or $\mathcal{Y}=(Y_l+Y_0)/2$, or $\mathcal{Y}=$constant, the volume integral of $D(\mathcal{Y})$ and $M(\mathcal{Y})$ for the whole space vanishes, i.e.,

$$\left.\begin{aligned}\sum_i\sum_j\sum_k D(\mathcal{Y})\cdot\Delta V_{ijk}=0\\ \sum_i\sum_j\sum_k M(\mathcal{Y})\cdot\Delta V_{ijk}=0\end{aligned}\right\} \quad (2.12)$$

under the boundary conditions: $\bar{\omega}=0$ at the top and the bottom of the atmosphere. With the same condition on $\mathcal{Y}$, the global area integral of $H_1(\mathcal{Y})$ and $N_1(\mathcal{Y})$ also vanishes,

$$\left.\begin{aligned}\sum_i\sum_j H_1(\mathcal{Y})\cdot\Delta S_{ij}=0\\ \sum_i\sum_j N_1(\mathcal{Y})\cdot\Delta S_{ij}=0\end{aligned}\right\} \quad (2.13)$$

(2) The global area integrals of $H_2(Y)$ and $N_2(Y)$ become zero,

$$\left.\begin{aligned}\sum_i\sum_j H_2(Y)\cdot\Delta S_{ij}=0\\ \sum_i\sum_j N_2(Y)\cdot\Delta S_{ij}=0\end{aligned}\right\} \quad (2.14)$$

(3) The relations below also follow,

$$\left.\begin{aligned}A_0\cdot D\left(\frac{A_l+A_0}{2}\right)=\frac{A_0^2}{2}D(1)+D\left(\frac{A_lA_0}{2}\right)\\ A_0\cdot M\left(\frac{A_l+A_0}{2}\right)=\frac{A_0^2}{2}M(1)+M\left(\frac{A_lA_0}{2}\right)\end{aligned}\right\} \quad (2.15)$$

$$L_\lambda(B,A)=G_\lambda(AB)-A_0G_\lambda(B) \quad (2.16)$$

$$L_\theta(B,A)=G_\theta(AB)-A_0G_\theta(B) \quad (2.17)$$

$$u_0G_\lambda(P_*A)+v_0G_\theta(P_*A)=H_2(A)-A_0H_1(1)+A_0[u_0G_\lambda(P_*)+v_0G_\theta(P_*)] \quad (2.18)$$

These relations correspond to the following differential formulas:

For (2.15) we have

$$A\nabla_H\cdot(AP_*\mathbf{V}_H)=\frac{A^2}{2}\nabla_H\cdot(P_*\mathbf{V}_H)+\nabla_H\cdot\left(\frac{A^2}{2}P_*\mathbf{V}_H\right)$$

where $\mathbf{V}_H$ is the vector of the horizontal wind and ∇_H is the horizontal gradient operator in spherical coordinates.

For (2.16) and (2.17), we have

$$B\nabla_HA=\nabla_H(AB)-A\nabla_HB$$

For (2.18),

$$\mathbf{V}_H\cdot\nabla_H(P_*A)=\nabla_H\cdot(P_*A\mathbf{V}_H)-A\nabla_H\cdot(P_*\mathbf{V}_H)+A\mathbf{V}_H\cdot\nabla_HP_*$$

3. FINITE-DIFFERENCE FORMS OF THE SYSTEM OF PRIMITIVE EQUATIONS

The equations of motion in λ, θ, σ coordinates are written

$$\frac{\partial}{\partial t}(P_*u)=-\mathcal{D}_3(u)+\left(f+\frac{\tan\theta}{a}u\right)P_*v-R\cdot\frac{\partial P_*T}{\alpha\partial\lambda}-\frac{\partial}{\partial\sigma}\left(P_*\sigma\frac{\partial\phi}{\alpha\partial\lambda}\right)+F_\lambda \quad (3.1)$$

$$\frac{\partial}{\partial t}(P_*v)=-\mathcal{D}_3(v)-\left(f+\frac{\tan\theta}{a}u\right)P_*u-R\cdot\frac{\partial P_*T}{a\partial\theta}-\frac{\partial}{\partial\sigma}\left(P_*\sigma\frac{\partial\phi}{a\partial\theta}\right)+F_\theta \quad (3.2)$$

where f is the Coriolis parameter; R, the gas constant for dry air; T, temperature; ϕ, geopotential of a sigma surface; and F_λ and F_θ, frictional forces in the zonal and meridional directions respectively. The first law of thermodynamics is written

$$\frac{\partial}{\partial t}(P_*T)=-\mathcal{D}_3(T)+\frac{R}{c_p}\cdot\frac{T\omega}{\sigma}+\frac{P_*\dot{q}}{c_p}+F_T \quad (3.3)$$

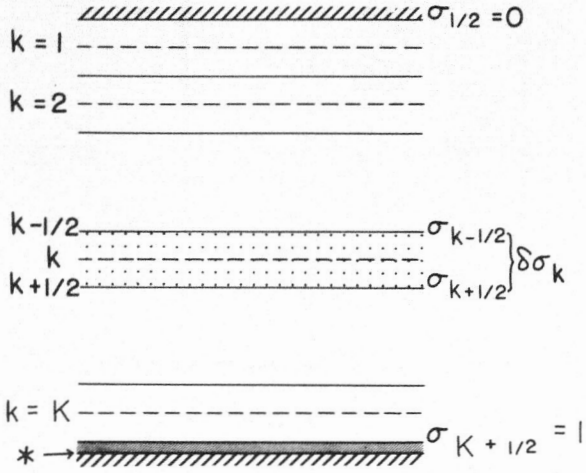

FIGURE 4.—Diagram of the vertical division of the model atmosphere into "K" layers centered at k sigma levels and bounded by $\sigma_{k+\frac{1}{2}}$ and $\sigma_{k-\frac{1}{2}}$. Star (*) level is the ground surface, and the top of the atmosphere is at $\sigma_{\frac{1}{2}}=0$.

where c_p is the specific heat capacity at constant pressure; ω, vertical P-velocity (dP/dt); $\dot{q}$, added heat per unit mass; and F_T, the effect of thermal diffusion. The continuity equation takes either of the forms (3.4) and (3.5)

$$\frac{\partial}{\partial t}P_*=-\mathcal{D}_3(1) \tag{3.4}$$

or

$$\frac{\partial}{\partial t}P_*=-\int_0^1 \mathcal{D}_2(1)\,d\sigma \tag{3.5}$$

The vertical sigma- and P-velocities are to be obtained by the diagnostic relations (3.6) and (3.7) below. (See reference [4].)

$$\bar{\omega}=\frac{1}{P_*}\left[\sigma\int_0^1 \mathcal{D}_2(1)\,d\sigma-\int_0^\sigma \mathcal{D}_2(1)\,d\sigma\right] \tag{3.6}$$

$$\omega=P_*\bar{\omega}+\sigma\left[\frac{\partial P_*}{\partial t}+u\,\frac{\partial P_*}{a\partial\lambda}+v\,\frac{\partial P_*}{a\partial\theta}\right] \tag{3.7}$$

The relation (3.8) below gives the hydrostatic relation.

$$\frac{\partial\phi}{\partial\sigma}=-\frac{RT}{\sigma}\quad\text{or}\quad \phi-RT=\frac{\partial\phi\sigma}{\partial\sigma} \tag{3.8}$$

Figure 4 shows the vertical division of the air column into K layers and the assignment of a k index to each level. We assume that the variables u, v, T, and ω are given for the levels having integer k, while ϕ, $\bar{\omega}$, and σ are for the levels with half-integer k. (See fig. 3.) The surface pressure P_* is, of course, independent of k.

VERSION I OF THE FINITE-DIFFERENCE FORMS

The above prognostic equations (3.1) through (3.5) are approximated by means of the finite-difference operators defined in the previous section as follows.

$$\frac{\partial}{\partial t}(P_{*0}u_0)=-D\left(\frac{u_1+u_0}{2}\right)+(\hat{f}+\hat{m}u_0)P_{*0}v_0 -RG_\lambda(P_*T)-\frac{\delta_k[\sigma\cdot L_\lambda(P_*,\phi)]}{\delta_k\sigma}+(F_\lambda)_0 \tag{3.1A}$$

$$\frac{\partial}{\partial t}(P_{*0}v_0)=-D\left(\frac{v_1+v_0}{2}\right)-(\hat{f}+\hat{m}u_0)P_{*0}u_0 -RG_\theta(P_*T)-\frac{\delta_k[\sigma\cdot L_\theta(P_*,\phi)]}{\delta_k\sigma}+(F_\theta)_0 \tag{3.2A}$$

$$\frac{\partial}{\partial t}(P_{*0}T_0)=-D\left(\frac{T_1+T_0}{2}\right)+\frac{R}{c_p}\cdot\frac{T_0\omega_0}{\frac{1}{2}(\sigma_{k+1/2}+\sigma_{k-1/2})} +\frac{P_{*0}}{c_p}\hat{\dot{q}}+(F_T)_0 \tag{3.3A}$$

$$\frac{\partial}{\partial t}P_{*0}=-D(1) \tag{3.4A}$$

or

$$\frac{\partial}{\partial t}P_{*0}=-\sum_{k=1}^{K}H_1(1)\Delta_k\sigma \tag{3.5A}$$

where

$$\hat{f}=\frac{1}{\Delta V}\iiint_{\Delta V} f\,dV=2\Omega\sin\theta_{ij}\cos(\Delta\theta_{ij}/2)$$

where Ω=angular velocity of the rotation of the earth.

$$\hat{m}=\frac{1}{\Delta V}\iiint_{\Delta V}\frac{\tan\theta}{a}\,dV=\frac{\tan\theta_{ij}}{a}$$

$$\hat{\dot{q}}=\frac{1}{\Delta V}\iiint_{\Delta V}\dot{q}\,dV$$

The diagnostic relations corresponding to (3.6) to (3.8) are

$$\bar{\omega}_{k+1/2}=\frac{1}{P_{*0}}\left[\sigma_{k+1/2}\sum_{k'=1}^{K}\{H_1(1)\Delta_{k'}\sigma\}-\sum_{k'=1}^{k}\{H_1(1)\Delta_{k'}\sigma\}\right] \tag{3.6A}$$

$$\omega_{0k}=P_{*0}\cdot\frac{\bar{\omega}_{k+1/2}+\bar{\omega}_{k-1/2}}{2} +\frac{\sigma_{k+1/2}+\sigma_{k-1/2}}{2}\left[\frac{\partial P_{*0}}{\partial t}+u_0G_\lambda(P_*)+v_0G_\theta(P_*)\right] \tag{3.7A}$$

$$\frac{\delta_k\phi}{\delta_k\sigma}=-\frac{RT_k}{\frac{1}{2}(\sigma_{k+1/2}+\sigma_{k-1/2})}\quad\text{or}\quad \phi_k-RT_k=\frac{\delta_k(\phi\sigma)}{\delta_k\sigma} \tag{3.8A}$$

where ϕ_k has to be related to $\phi_{k+\frac{1}{2}}$ or $\phi_{k-\frac{1}{2}}$ by (3.9)

$$\phi_{k\pm1/2}=\phi_k\mp\frac{\Delta_k\sigma}{2}\cdot\frac{RT_k}{\frac{1}{2}(\sigma_{k+1/2}+\sigma_{k-1/2})} \tag{3.9}$$

where $\Delta_k\sigma=\sigma_{k+1/2}-\sigma_{k-1/2}$. Relation (3.9) insures that

$$\phi_k=\tfrac{1}{2}(\phi_{k+1/2}+\phi_{k-1/2}) \tag{3.10}$$

The last terms in (3.1A), (3.2A), and (3.3A) will be developed in Appendix 1.

Condition (2.12) guarantees the conservation of total mass of the air in (3.4A).

Notice that the vertical summations (weighted by $\Delta_k\sigma/g$) of the next-to-last terms on the right-hand sides of (3.1A) and (3.2A) take the values $-L_\lambda(P_*, z_*)$ and $-L_\theta(P_*, z_*)$, where z_* is the height of the earth's surface above mean sea level. These values evaluate the effect of mountains on the integrated momentum of the air column. If the boxes are linked to form a ring along a latitude circle as in this study, the relation (3.11) below is true.

$$\sum_i \cos\theta_{ij} G_\lambda(P_* T)\Delta S_{ij}=0 \tag{3.11}$$

Consequently, in this case the pressure gradient force contributes to the budget of total absolute angular momentum only through the mountain torque.

The differential form which seems suitable for representing the budget of relative angular momentum is derived from (3.1) by using the relation

$$\alpha\left[-\mathcal{D}_3(u)+\frac{\tan\theta}{a}P_* uv\right]=-\mathcal{D}_3(\alpha u) \tag{3.12}$$

Furthermore, the following relation is used to obtain an appropriate form of the budget of absolute angular momentum,

$$\alpha f P_* v=-\mathcal{D}_3(\alpha^2\Omega)-\frac{\partial P_*\alpha^2\Omega}{\partial t} \tag{3.13}$$

Examining (3.1A), we see that the finite-difference analog to the above conditions is not satisfied exactly. However, based on the results of the angular momentum analysis of the general circulation experiment [4] at the Geophysical Fluid Dynamics Laboratory (GFDL) of ESSA, the truncation errors in this respect are supposedly not cumulative so that the numerical completeness in the budget of angular momentum is held to a high degree of approximation.

A complete system of primitive equations is formed by the relations (3.1A) through (3.8A) together with the boundary condition (3.14):

$$\bar{\omega}_{1/2}=0, \quad \bar{\omega}_{K+1/2}=0 \tag{3.14}$$

In addition, if use is made of the above-mentioned version of the finite-difference form, the relation to be derived from (3.4), i.e.,

$$\frac{\partial}{\partial t}\left(\frac{P_*^2}{2}\right)=-\left(\frac{P_*^2}{2}\right)\nabla\cdot\mathbf{V}-\nabla\cdot(\mathbf{V}P_*^2/2)$$

also holds numerically.

VERSION II OF THE FINITE-DIFFERENCE FORMS

Another version of the finite-difference forms of the primitive equations can be developed. In this version, the terms of pressure gradient force in the momentum equations are transformed so that these terms take the forms,

$$\left\{-RT\frac{\partial P_*}{\alpha\partial\lambda}-P_*\frac{\partial\phi}{\alpha\partial\lambda}\right\}$$

instead of

$$\left\{-R\frac{\partial P_* T}{\alpha\partial\lambda}-\frac{\partial}{\partial\sigma}\left(P_{*\sigma}\frac{\partial\phi}{\alpha\partial\lambda}\right)\right\}$$

in (3.1) and

$$\left\{-RT\frac{\partial P_*}{a\partial\theta}-P_*\frac{\partial\phi}{a\partial\theta}\right\}$$

instead of

$$\left\{-R\frac{\partial P_* T}{a\partial\theta}-\frac{\partial}{\partial\sigma}\left(P_{*\sigma}\frac{\partial\phi}{a\partial\theta}\right)\right\}$$

in (3.2).

Then a system of finite-difference equations can be established by changing the forms of pressure gradient force terms from those in (3.1A) and (3.2A) to

$$-RT_0 G_\lambda(P_*)-P_{*0}G_\lambda(\phi)$$

and

$$-RT_0 G_\theta(P_*)-P_{*0}G_\theta(\phi)$$

respectively, and by replacing D- and H_1-operators in (3.1A) through (3.8A) by M- and N_1-operators defined in the previous section. In addition, the relation (3.9) and the boundary condition (3.14) are required to complete the system of equations.

By means of (3.8A), the finite-difference form of the pressure gradient force for the λ-direction in this version can be rewritten as follows

$$-RT_0 G_\lambda(P_*)-P_{*0}G_\lambda(\phi)=-E_\lambda(\phi P_*)+E_\lambda\left(\frac{\delta_k(\phi\sigma)}{\delta_k\sigma}P_*\right)-\frac{\delta_k[\sigma P_{*0}G_\lambda(\phi)]}{\delta_k\sigma} \tag{3.15}$$

If boxes are placed along a latitude circle to form a ring, the summation $\sum_i \cos\theta_{ij}E_\lambda(AB)\Delta S_{ij}$ equals zero. Therefore, in this case, the volume integral of the term for the pressure gradient force does not reveal the presence of a fictitious source of momentum but contains only the effect of mountain torque resulting from the third term on the right-hand side of (3.15). In this respect, there is no difference between the two versions of the finite-difference forms. However, in an analysis of the momentum budget, Version I seems to be more suitable since the effect of mountain torque is explicitly shown by it, and this effect can be directly estimated for an air column.

Regarding the conservation of air mass and budget of relative and absolute angular momentum, Version II has the same characteristics as Version I.

Because of the circumstances of computer programing, we used the difference equations written in Version II in our test integration of the equations for a general circulation model.

4. FINITE-DIFFERENCE FORMS OF THE ENERGY EQUATIONS

ENERGY BUDGET FOR VERSION I

In our derivation of the energy equations corresponding to the system of primitive equations, the differential forms of the equations are considered first. The equation for the change of kinetic energy is obtained from (3.1), (3.2), and (3.4) by using the relation (4.1):

$$\frac{\partial}{\partial t}\left(P_*\frac{u^2+v^2}{2}\right)=u\frac{\partial}{\partial t}(P_*u)+v\frac{\partial}{\partial t}(P_*v)-\frac{u^2+v^2}{2}\frac{\partial P_*}{\partial t} \quad (4.1)$$

On the other hand, by use of (3.4), (3.7), and (3.8), the following relation is derived:

$$-u\left[R\frac{\partial P_*T}{\alpha\partial\lambda}+\frac{\partial}{\partial\sigma}\left(P_{*\sigma}\frac{\partial\phi}{\alpha\partial\lambda}\right)\right]-v\left[R\frac{\partial P_*T}{a\partial\theta}+\frac{\partial}{\partial\sigma}\left(P_{*\sigma}\frac{\partial\phi}{a\partial\theta}\right)\right]=-\mathcal{D}_3(\phi)-\frac{\partial\phi\sigma}{\partial\sigma}\frac{\partial P_*}{\partial t}-R\frac{T\omega}{\sigma} \quad (4.2)$$

Consequently, the following equation for kinetic energy is obtained:

$$\frac{\partial}{\partial t}\left(P_*\frac{u^2+v^2}{2}\right)=-\mathcal{D}_3\left(\frac{u^2+v^2}{2}+\phi\right)-\frac{\partial\phi\sigma}{\partial\sigma}\frac{\partial P_*}{\partial t}-R\frac{T\omega}{\sigma}+uF_\lambda+vF_\theta \quad (4.3)$$

In order to derive the potential energy equation the relation (3.3) is first multiplied by c_p as follows:

$$\frac{\partial}{\partial t}(P_*c_pT)=-\mathcal{D}_3(c_pT)+R\frac{T\omega}{\sigma}+P_*\dot{q}+c_pF_T \quad (4.4)$$

The quantity c_pT is related to the internal plus potential energy, i.e., $c_vT+\phi$, through (3.8)

$$c_pT=c_vT+RT=c_vT+\phi-\frac{\partial\phi\sigma}{\partial\sigma}$$

Accordingly, we derive the following:

$$\frac{\partial}{\partial t}\int_0^1 P_*c_pT\frac{d\sigma}{g}=\frac{\partial}{\partial t}\int_0^1 P_*(c_vT+\phi)\frac{d\sigma}{g}-\frac{\phi_*}{g}\frac{\partial P_*}{\partial t} \quad (4.5)$$

The vertical integral of the sum of (4.3) and (4.4) becomes, therefore,

$$\frac{\partial}{\partial t}\int_0^1 P_*\left(c_vT+\phi+\frac{u^2+v^2}{2}\right)\frac{d\sigma}{g}=-\int_0^1\mathcal{D}_2\left(c_pT+\phi+\frac{u^2+v^2}{2}\right)\frac{d\sigma}{g}+\int_0^1(uF_\lambda+vF_\theta+P_*\dot{q}+c_pF_T)\frac{d\sigma}{g} \quad (4.6)$$

The change of the total energy of the atmosphere is given by the area integral of (4.6):

$$\frac{\partial}{\partial t}\iiint P_*\left(c_vT+\phi+\frac{u^2+v^2}{2}\right)\frac{dV}{g}=\iiint(uF_\lambda+vF_\theta+P_*\dot{q}+c_pF_T)\frac{dV}{g} \quad (4.7)$$

In (4.7), the volume integral of $(uF_\lambda+vF_\theta)$ represents the internal dissipation of kinetic energy and the work done by the wind against the surface stress, $\dot{q}$ contains the effects of radiation and condensation, and the volume integral of c_pF_T gives the diffusive exchange of sensible heat at the air-earth boundary.

The finite-difference form of the kinetic energy equation corresponding to the above differential form is easily obtained by the relation:

$$\frac{\partial}{\partial t}\left(P_{*0}\frac{u_0^2+v_0^2}{2}\right)=u_0\frac{\partial}{\partial t}(P_{*0}u_0)+v_0\frac{\partial}{\partial t}(P_{*0}v_0)-\frac{u_0^2+v_0^2}{2}\cdot\frac{\partial P_{*0}}{\partial t} \quad (4.1A)$$

We can derive (4.2A) with the use of (2.4), (2.16), (2.17), (2.18), (3.4A), (3.7A), (3.8A), and (3.9),

$$-u_0\left\{RG_\lambda(P_*T)+\frac{1}{\delta_k\sigma}\delta_k[\sigma\cdot L_\lambda(P_*,\phi)]\right\}-v_0\left\{RG_\theta(P_*T)+\frac{1}{\delta_k\sigma}\delta_k[\sigma\cdot L_\theta(P_*,\phi)]\right\}=-H_2(\phi_k)-\frac{\delta_k(P_{*0}\phi\bar{\omega})}{\delta_k\sigma}-\frac{\delta_k(\phi\sigma)}{\delta_k\sigma}\frac{\partial P_{*0}}{\partial t}-R\frac{T_0\omega_0}{\frac{1}{2}(\sigma_{k+\frac{1}{2}}+\sigma_{k-\frac{1}{2}})} \quad (4.2A)$$

By use of (4.2A), the finite-difference form of the kinetic energy equation becomes

$$\frac{\partial}{\partial t}\left(P_{*0}\frac{u_0^2+v_0^2}{2}\right)=-D\left(\frac{u_lu_0+v_lv_0}{2}\right)-H_2(\phi_k)-\frac{\delta_k(P_{*0}\phi\bar{\omega})}{\delta_k\sigma}-\frac{\delta_k(\phi\sigma)}{\delta_k\sigma}\frac{\partial P_{*0}}{\partial t}-R\frac{T_0\omega_0}{\frac{1}{2}(\sigma_{k+\frac{1}{2}}+\sigma_{k-\frac{1}{2}})}+u_0(F_\lambda)_0+v_0(F_\theta)_0 \quad (4.3A)$$

Notice that the volume integral of the first, second, and third terms on the right-hand side of (4.3A) vanishes as shown by (2.12), (2.14), and (3.14), respectively.

The finite-difference form of (4.4) is easily obtained.

$$\frac{\partial}{\partial t}(P_{*0}c_pT_0)=-D\left(c_p\frac{T_l+T_0}{2}\right)+R\frac{T_0\omega_0}{\frac{1}{2}(\sigma_{k+\frac{1}{2}}+\sigma_{k-\frac{1}{2}})}+P_{*0}\hat{\dot{q}}+c_p(F_T)_0 \quad (4.4A)$$

From the hydrostatic relation (3.8A),

$$c_pT_0=c_vT_0+RT_0=c_vT_0+\phi_0-\frac{\delta_k(\phi\sigma)}{\delta_k\sigma}$$

and consequently,

$$\frac{\partial}{\partial t}\left[\sum_{k=1}^{K}P_{*0}c_pT_0\frac{\delta_k\sigma}{g}\right]=\frac{\partial}{\partial t}\left[\sum_{k=1}^{K}P_{*0}(c_vT_0+\phi_0)\frac{\delta_k\sigma}{g}\right]-\frac{\phi_{*0}}{g}\cdot\frac{\partial P_{*0}}{\partial t} \quad (4.5A)$$

The following equation for the change of total energy of the air column is derived from (4.3A), (4.4A), and (4.5A):

$$\frac{\partial}{\partial t}\left[\sum_{k=1}^{K} P_{*0}\left(c_v T_0+\phi_0+\frac{u_0^2+v_0^2}{2}\right)\frac{\delta_k\sigma}{g}\right]$$
$$=-\sum_{k=1}^{K} H_1\left(c_p\frac{T_l+T_0}{2}+\frac{u_l u_0+v_l v_0}{2}\right)\frac{\delta_k\sigma}{g}-\sum_{k=1}^{K} H_2(\phi_k)\frac{\delta_k\sigma}{g}$$
$$+\sum_{k=1}^{K}\{u_0(F_\lambda)_0+v_0(F_\theta)_0+P_{*0}\hat{\dot{q}}+c_p(F_T)_0\}\frac{\delta_k\sigma}{g} \quad (4.6A)$$

Integrating (4.6A) over the entire domain by means of (2.13) and (2.14), we obtain an equation which corresponds exactly to (4.7),

$$\frac{\partial}{\partial t}\left[\sum_i\sum_j\sum_{k=1}^{K}\left\{P_{*0}\left(c_v T_0+\phi_0+\frac{u_0^2+v_0^2}{2}\right)\frac{\Delta V_{ijk}}{g}\right\}\right]$$
$$=\sum_i\sum_j\sum_{k=1}^{K}[u_0(F_\lambda)_0+v_0(F_\theta)_0+P_{*0}\hat{\dot{q}}+c_p(F_T)_0]\frac{\Delta V_{ijk}}{g} \quad (4.7A)$$

The finite-difference form of (4.7) above shows that there exists no fictitious source of energy in this scheme, and our finite-difference forms, Version I, of the primitive equations, are thus energetically consistent provided that time truncation error can be disregarded.

ENERGY BUDGET FOR VERSION II

The finite-difference forms of the energy equations for Version II in the previous section are to be derived by the same procedure as used for Version I. The relations corresponding to (4.3A), (4.4A), and (4.6A) are obtained by replacing D-, H_1-, and H_2-operators in these formulas by M-, N_1-, and N_2-operators, respectively. The area integral of the relation expressing the change of total energy for an air column yields the formula which is exactly equivalent to (4.7A). Consequently, the Version II system of equations in Section 3 is also consistent from the energetical point of view.

5. RESULTS OF THE TEST COMPUTATION

Our main purpose in establishing the finite-difference scheme based on the box method is to apply it to a spherical grid system to develop a numerical experiment of the general circulation on a global scale. As a test of the usefulness of the proposed schemes, we made the numerical integration of a system of primitive equations which are formulated in the form of Version II in section 3 for a nine-level general circulation model of the atmosphere.

The vertical division of the atmosphere into nine layers is only slightly changed from that used in the experiment [4]. See table 1. Figure 5 shows an octant of the grid system, in which the dots at the centers of the boxes represent the grid points. The horizontal cross-sections of the boxes are shown in this figure. The grid system is the same kind as the spherical grid system 1 proposed by Kurihara [2]. The resolution of the grid network is such that between the pole and the equator there are 24 points. As pointed out in [2], the distribution of grid points is chosen so that the resolution is nearly uniform with respect to the area.

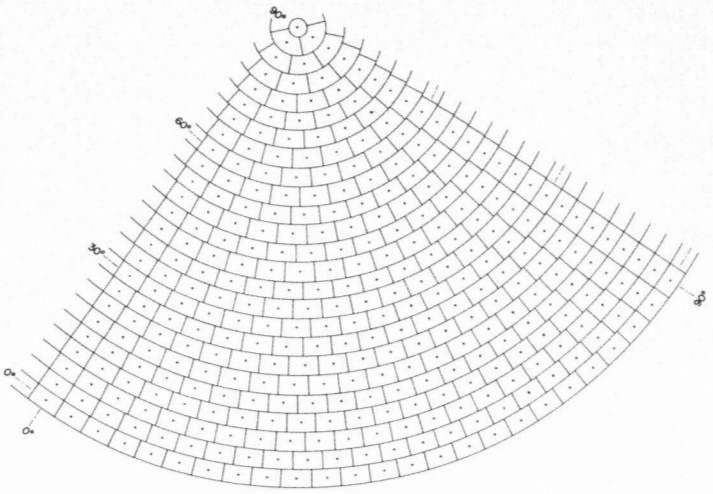

FIGURE 5.—Diagram of one octant of the grid system used in the test computation. Dots indicate the grid points located at the centers of the boxes. There are 24 grid points between the equator and the pole. The horizontal cross-sections of the boxes and the way they are positioned with respect to adjacent boxes are shown. Note that in this diagram latitudes are equally spaced which results in some distortion of box shapes, especially in the Tropics.

Note that, if we had adopted a grid similar to the system 3 in [2], we could have avoided having two polar boxes.

The system of fundamental equations is the same as that adopted in the general circulation experiment without hydrologic processes by Smagorinsky, Manabe, and Holloway [4], except for the form of the frictional dissipation and heat diffusion. Horizontal diffusion of momentum and of heat in our model are estimated primarily by a simplified form of the so-called linear viscosity. The value of the kinematical eddy viscosity coefficient used was 5×10^9 cm.^{2} sec.$^{-1}$ before the 6th day of the integration and 10^9 cm.^{2} sec.$^{-1}$ afterward.

The diffusion of momentum in the vertical direction was computed by means of an eddy viscosity coefficient which depends on mixing length. This was identical with the vertical diffusion used in the model of reference [4]. The stabilizing effects of moist convection are implicitly simulated in our model in the same manner as was done in [4] by

TABLE 1.—*Vertical leveling of model*

Level k	Sigma	Height in km. (Standard Atmosphere)
0.5	0	infinity
1.0	0.010	30.77
1.5	.020	24.10
2.0	.060	19.88
2.5	.100	15.65
3.0	.165	13.15
3.5	.230	10.65
4.0	.315	8.83
4.5	.400	7.02
5.0	.500	5.55
5.5	.600	4.08
6.0	.685	3.11
6.5	.770	2.14
7.0	.835	1.51
7.5	.900	.87
8.0	940	.52
8.5	.980	.17
9.0	.990	.08
9.5	1.000	.00

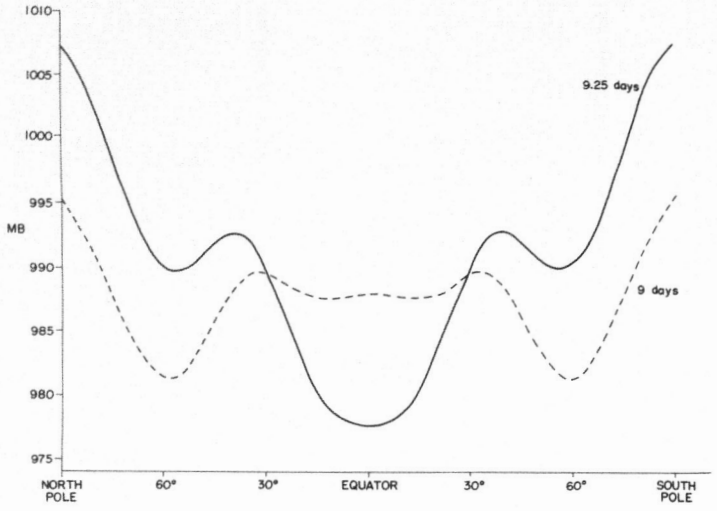

FIGURE 6.—Latitudinal distribution of zonal mean surface pressure at 9 and 9.25 days. The mean surface pressure of the model atmosphere is about 28 mb. lower than observed because the model has the same mass of air as the actual atmosphere but it has no mountains.

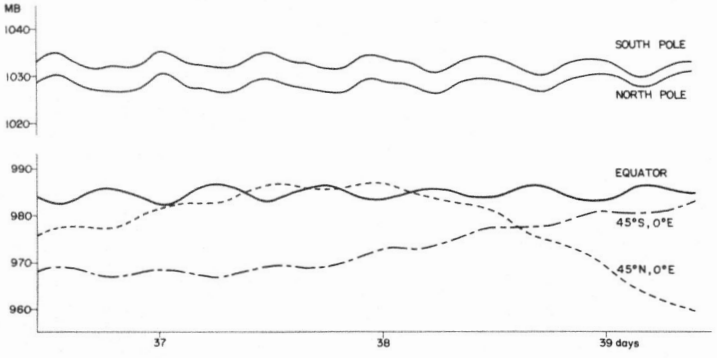

FIGURE 7.—Three-day time series of surface pressure at the north and south poles and at the intersections of 0° E. longitude with 45° N., 45° S., and the Equator. Since the surface is flat and uniform, the assignment of the location of the prime meridian is arbitrary.

adjusting the lapse rate to the moist adiabatic value, if the former exceeds the latter, without changing the mean temperature of any column of air.

Since the domain for which the calculations are made is global, no lateral boundary conditions are needed. The upper and lower boundary conditions, including the formulation of the air-earth interactions, are the same as used in [4]. The lower boundary is everywhere uniform and at sea level.

The scheme of time integration, including the use of an implicit integration scheme for the vertical diffusion terms, and the method of periodic time smoothing are the same as that used in the experiment [4], except that the time interval is 7.5 min. in the present model.

In the formulation of the radiational heating, the distribution of solar insolation and atmospheric absorbers such as water vapor, carbon dioxide, ozone, and cloud are assumed to be the same as those adopted in the experiment for a hemispheric domain [4]. They are extended symmetrically into the Southern Hemisphere across the equator.

The initial conditions for the test run are symmetric about the equator since time and zonal averages of the zonal component of winds, temperatures, and pressures for the last 70 days of the so-called dry general circulation model run [4] are given in each hemisphere. That is, the input data do not vary with longitude. Since the meridional wind component was small in the mean, it was set to zero initially in our run. As the only factor to destroy the symmetry between hemispheres and zonal uniformity within each hemisphere, before the start of the run all the temperatures were perturbed by random numbers in a range within plus or minus 0.1°K. The computations were extended to 50 days without any special sign of computational trouble. The maps of the output, which are made by interpolating the spherical grid onto a rectangular grid in which the latitudes are evenly spaced, shows that baroclinic waves with wave number 5 to 7 developed. The predicted patterns of variables remained smooth, and the behavior of the disturbances was reasonable.

In the early stages of the integration, an oscillation of the surface pressure with a period of about 11.5 hr. was observed. The range of oscillation at the poles reached 15 mb. Figure 6 shows the latitudinal distribution of zonal mean surface pressure at 9 days and that at 6 hr. later. It is seen that the seiche of air took place in each hemisphere. Corresponding to this, a rather rough variation of total relative angular momentum with time was also obtained in contrast to a slow variation of total absolute angular momentum. We suppose that the above-mentioned oscillation was initiated from an imbalance in the initial conditions, which may have resulted from one or more causes. At a later period in the test run, the state of quasi-equilibrium among the accelerations in the meridional direction seems to have been approached. As shown in figure 7, the range of oscillation at the poles decreased to 3 mb. We can see the passage of large-scale disturbances in middle latitudes in the same figure.

In figures 8 through 12, global maps of various variables at 50 days are shown. As indicated by the time series of total kinetic energy, total absolute and relative angular momentum, and mean hemispheric temperature shown in figure 13, the state of the atmosphere at this time is still not close to the quasi-equilibrium. However, well-developed disturbances do appear in middle latitudes, and no violent motions occurred at the low latitudes. Note that all patterns are smooth and there is no indication of computational trouble. In the map of the meridional component of wind, the existence of cross-equatorial flow is noticeable, which might imply a possibly important role of this flow in the general circulation of the atmosphere. At 50 days there are still strong high-pressure areas over the poles with correspondingly low surface temperatures there. This is a phenomenon which occurs in all model

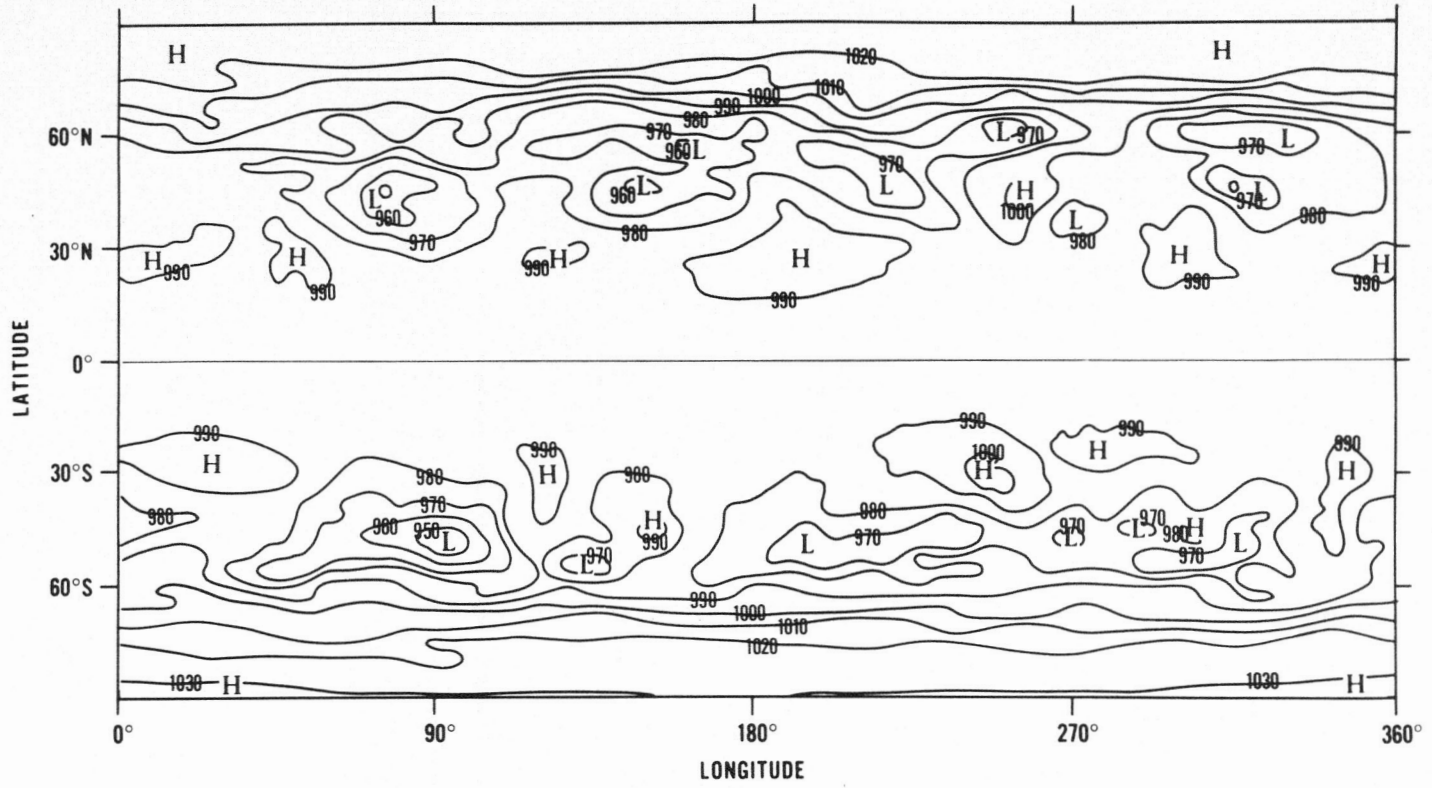

FIGURE 8.—Surface pressure map at 50 days. Contours are drawn every 10 mb. In this and the following maps, the latitudes are evenly spaced to the poles which occupy the entire top and bottom edges of the maps. The distortion at high latitudes is very great.

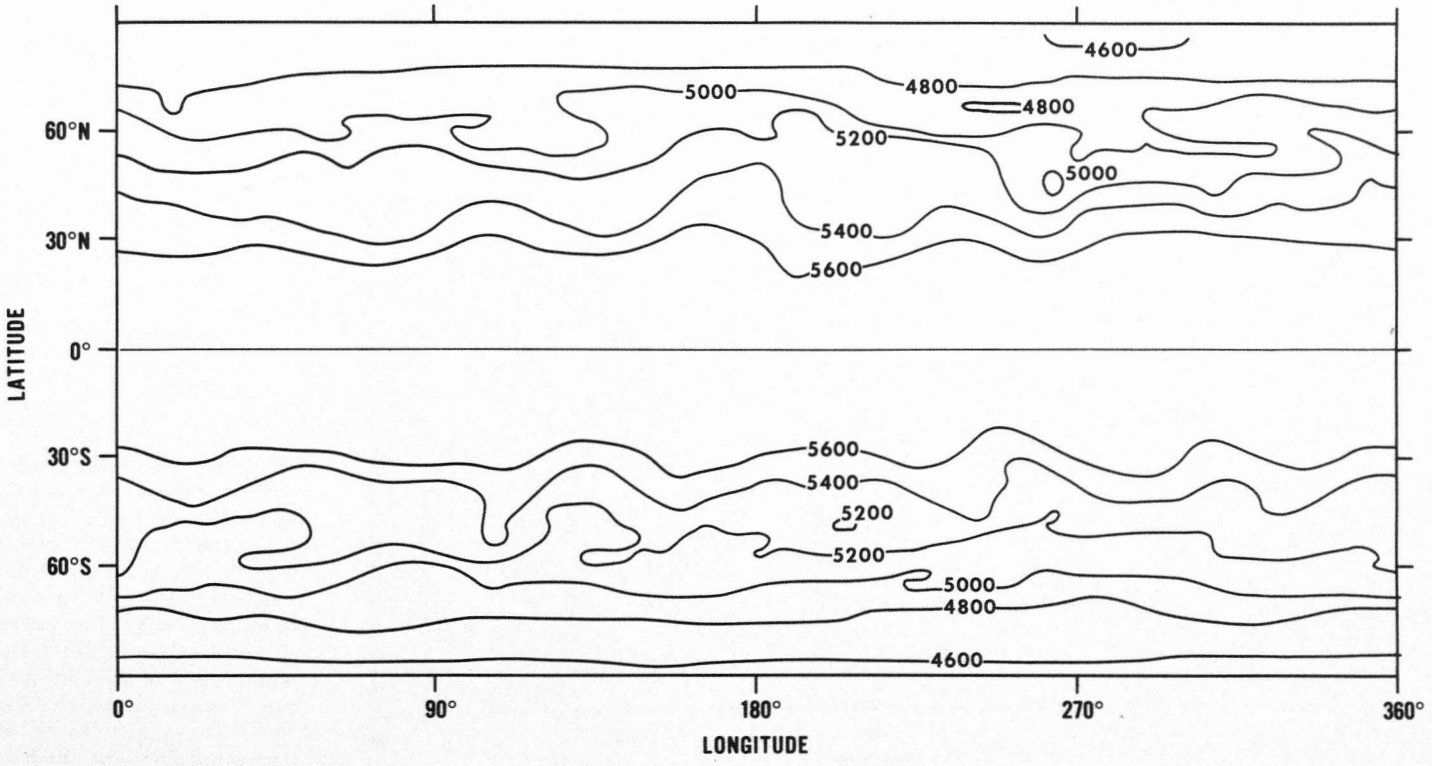

FIGURE 9.—Map of geopotential height at level 5 (approximately 500 mb.) at 50 days. Contours are drawn for every 200 m.

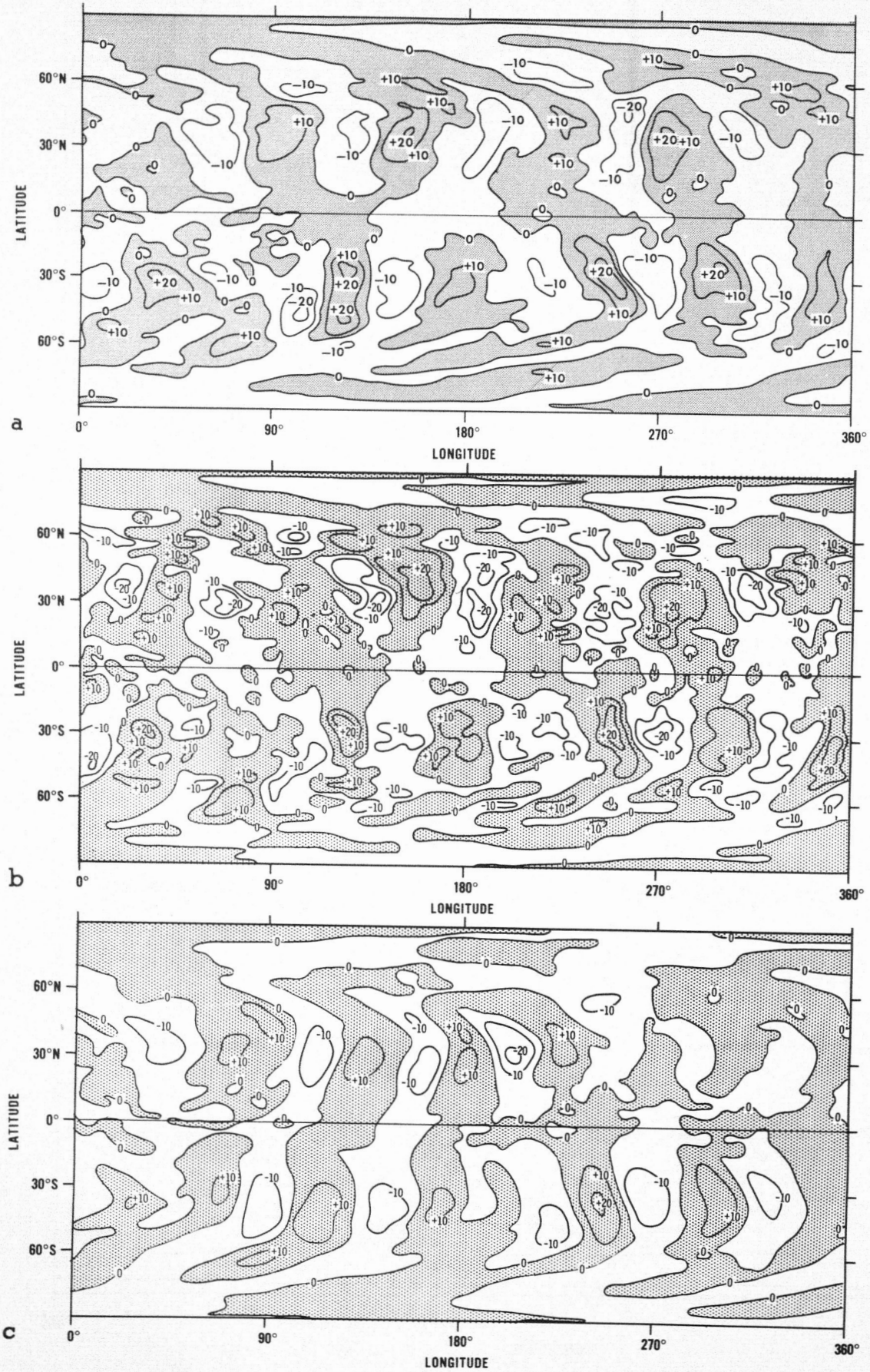

FIGURE 10.—Meridional component of the wind at level 5 at 50 days (a) for the standard run with linear viscosity and for the runs (b) with no viscosity and (c) with nonlinear viscosity. The latter two runs were started from 40-day data of the standard run. Contours are drawn for every 10 m./sec. Areas of northward flow are shaded.

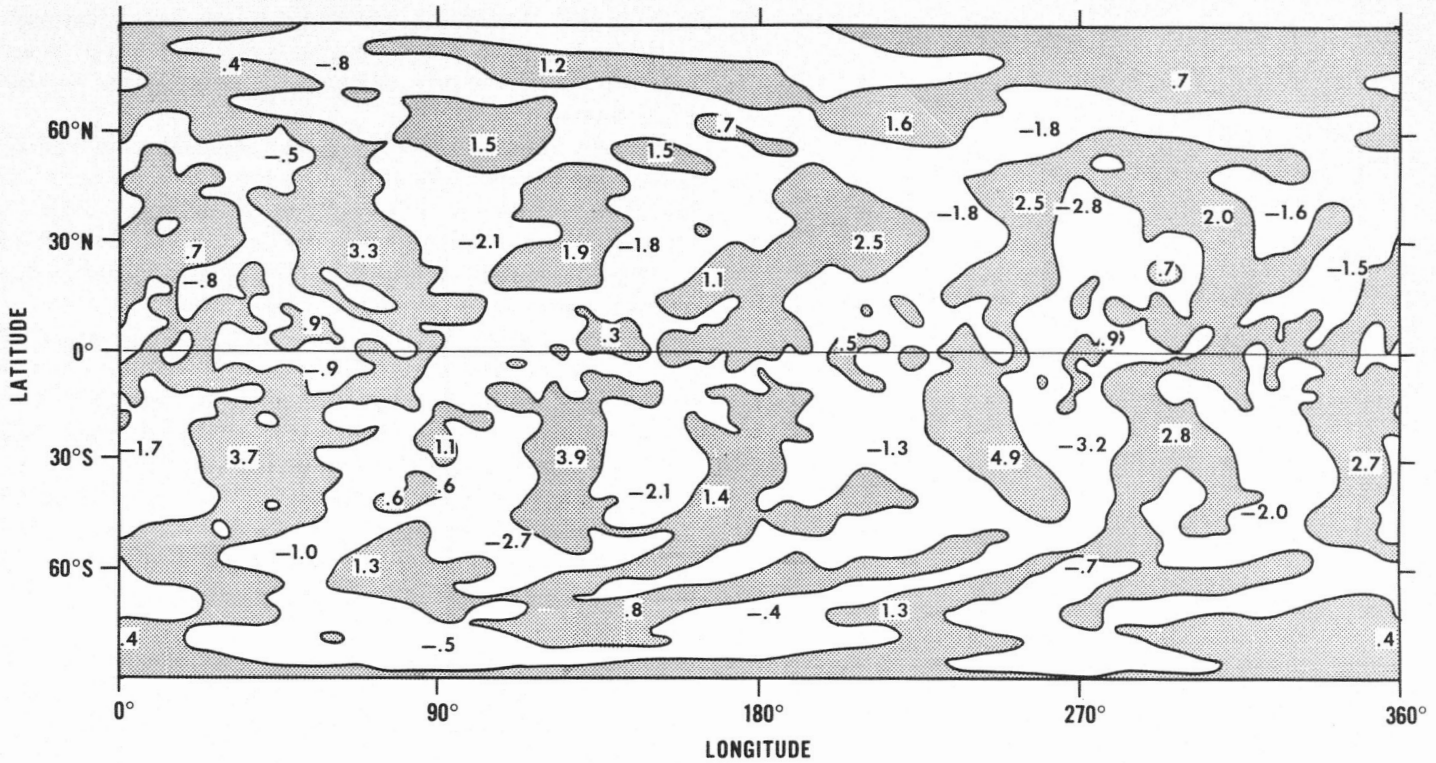

FIGURE 11.—Vertical velocity $\left(\omega = \frac{dP}{dt}\right)$ at level 5 at 50 days. Shaded areas are positive indicating sinking motion. Selected values are plotted on the map in microbars per second.

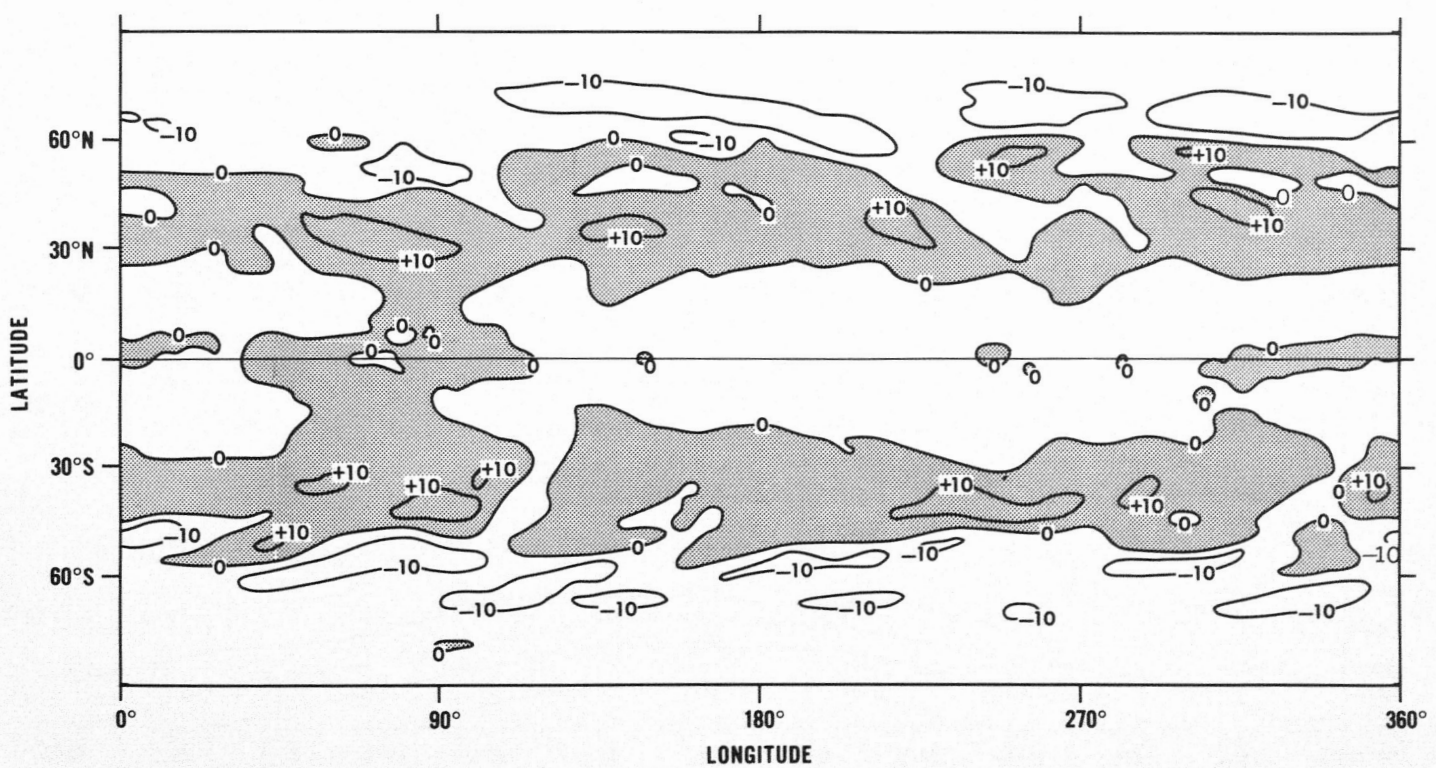

FIGURE 12.—Zonal component of the wind at level 9 (at approximately 990 mb. or 80 m. above the surface) at 50 days. Contours are drawn every 10 m./sec. Note the equatorial and polar easterlies and the westerlies (shaded) in middle latitudes.

269-089 O - 67 - 4

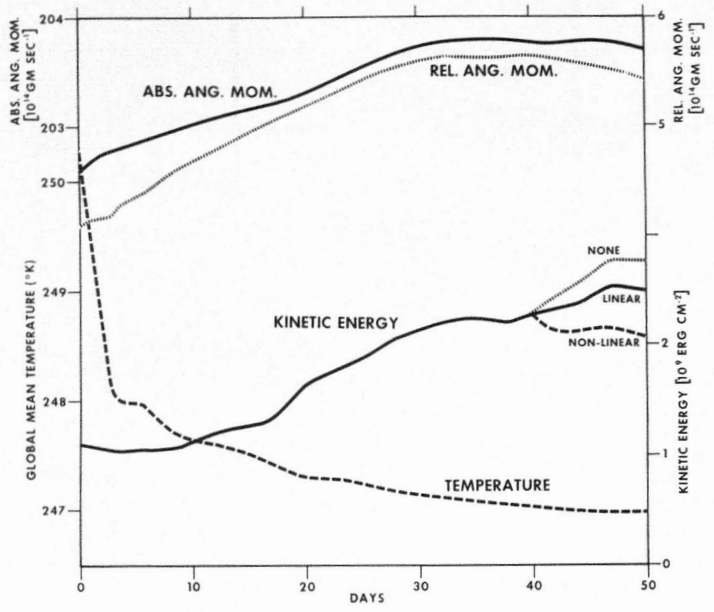

FIGURE 13.—Time series of global mean kinetic energy, absolute and relative angular momentum, and temperature for the 50-day test run. The 11.5-hr. oscillation was filtered out of the data by a two-weight running mean of values 46 time steps apart. Beyond 40 days the kinetic energy curve has three branches: one for the standard run with horizontal diffusion in the form of linear viscosity; a second for the test of the non-linear viscosity; and a third for the case with no horizontal diffusion at all.

experiments at GFDL during the early stages of their development. Later the baroclinic waves break through to the poles, raise polar temperatures, and lower polar pressures. We have not extended the computaion to this latter stage.

Cross-sections of the zonal mean of zonal wind and of zonal mean temperature at 45 days are shown in figure 14. Notice the jet stream at level 3 (about 165 mb.) at about 31°N. and 33°S., and the easterlies in the Tropics. There is a high degree of symmetry between hemispheres at this relatively early stage in the time integration.

The global mean kinetic energy is plotted in figure 15 along with the terms contributing to its change, i.e., the global mean of the conversion of potential energy to kinetic energy and the global mean total frictional dissipation of kinetic energy, for the 1-day period starting at day 45. The kinetic energy budget for this period is presented in table 2. These results support the discussions in section 4; i.e., the energy budget is consistently held by the system of equations used except for a small error resulting from time truncation.

The budget of global mean absolute angular momentum is given in table 3. The change in global mean absolute angular momentum from 45 to 46 days is insignificantly small. Accordingly, the product of mean global torque and the length of time indicates roughly the extent of the

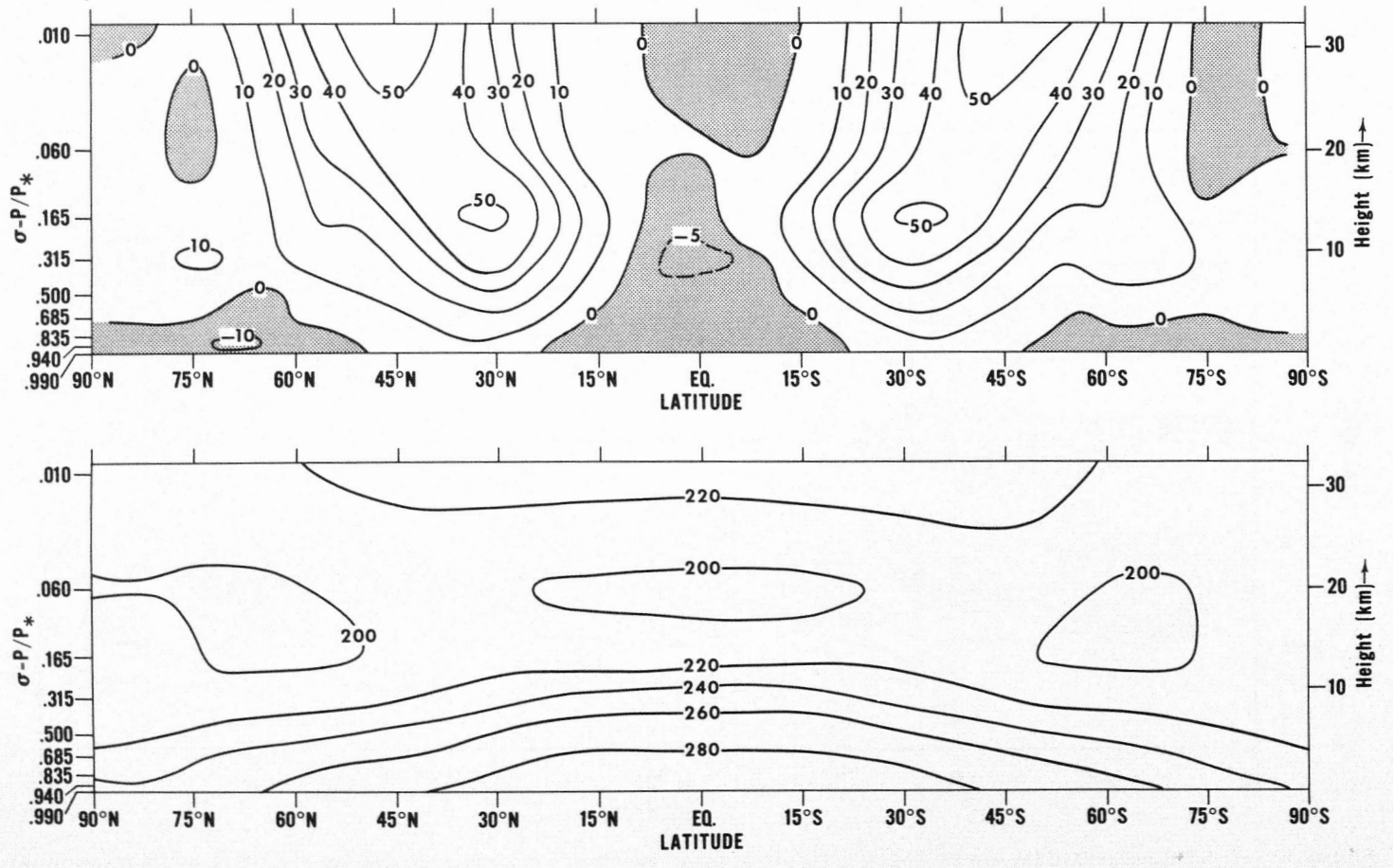

FIGURE 14.—Meridional cross-section at 45 days of (top) zonal mean zonal wind (m./sec.) and of (bottom)zonal mean temperature (° K.).

TABLE 2.—*Budget of kinetic energy for 45 to 46 days*

Kinetic energy at 46 days	2.486×10^{9} ergs cm.$^{-2}$
Kinetic energy at 45 days	2.412×10^{9} ergs cm.$^{-2}$
Rate of increase	0.074×10^{9} ergs cm.$^{-2}$ day^{-1}
Time mean global conversion	3130 ergs cm.$^{-2}$ sec.$^{-1}$
Time mean global dissipation	2200 ergs cm.$^{-2}$ sec.$^{-1}$
Net mean conversion	$\int$930 ergs cm.$^{-2}$ sec.$^{-1}$
	$\backslash 0.080\times10^{9}$ ergs cm.$^{-2}$ day^{-1}

TABLE 3.—*Budget of absolute angular momentum*

Absolute angular momentum at 46 days	2.0377035×10^{16} gm. sec.$^{-1}$
Absolute angular momentum at 45 days	2.0377000×10^{16} gm. sec.$^{-1}$
Rate of increase	$0.0000035\times10^{16}=3.5\times10^{10}$ gm. sec.$^{-1}$ day^{-1}
Time mean global torque	1.45×10^{7} dynes cm.$^{-1}$
Time integrated torque over 1-day period	125×10^{10} gm. sec.$^{-1}$

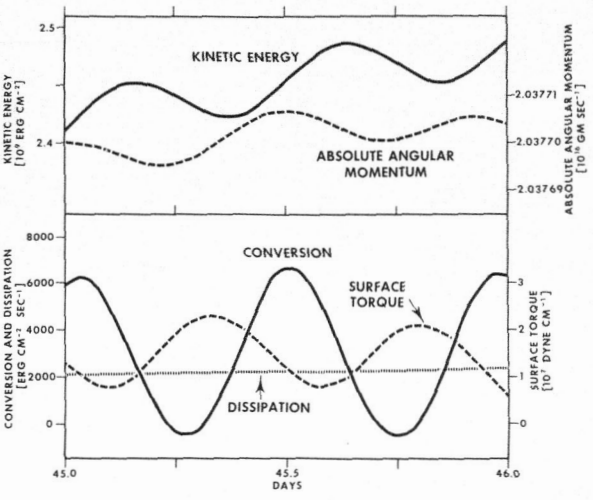

FIGURE 15.—Time series of global mean kinetic energy and absolute angular momentum together with terms contributing to their change; namely, conversion, dissipation, and surface torque, for the 1-day period starting at 45 days.

non-conservation of angular momentum in our model during this 1-day period. The mean torque error of about 10^{7} dynes/cm. is only a few percent of the magnitude of the mean surface torque in the Tropics or in middle latitudes. Therefore, this amount of error is practically negligible.

In general the development of flow in this numerical integration, such as the growth of baroclinic waves, appeared to be slow compared with the general circulation experiments by Smagorinsky, Manabe, and Holloway [4]. This might have been caused by the formulation of horizontal diffusion of momentum in the form of linear viscosity. In this case, diffusion is effective from the beginning of the run to make the flow smooth. If we had used a type of non-linear viscosity, the mixing of any given quantity would have been small until the deformation of the flow reached its normal level.

In order to investigate the differences in the behavior of the flow resulting from the different types of viscosity, two other test runs, one without any horizontal viscosity at all and another with non-linear viscosity, were started from the 40-day data, and the computations were continued for 10 days, in parallel with the standard run. In the run without viscosity, the flow accelerated and there was a marked reduction in the mean scale of the disturbances, but the integration remained stable without any catastrophic deterioration of the flow, and disturbances were still identifiable with ones found in the runs with viscosity. The surface pressure map and the distribution of meridional wind at level 5 (500 mb.) at 50 days are presented in figure 16 and in the middle part of figure 10, respectively, for comparison with the maps for the original test run having linear horizontal viscosity.

The surface pressure map at 50 days for the run in which the momentum diffusion in the form of non-linear viscosity was assumed after 40 days is presented in figure 17. The bottom part of figure 10 shows the meridional flow at level 5 for the same run. The contours are quite smooth, perhaps because of a large value of the coefficient in the expression for the non-linear viscosity. In figure 13, the variations of kinetic energy with time are plotted for the ten overlapping days during which the three different kinds of momentum diffusion were employed. In the case of the non-linear viscosity, the new level of kinetic energy seems to be about 10 percent lower than that for the case of linear viscosity. Examining the maps of surface pressure and the meridional wind at level 5, we infer that the differences in energy level can be attributed to changes in both the scale and the amplitude of the disturbances resulting from differences in the type of viscosity and in the value of the viscosity coefficient. The phase speed of disturbances is apparently also affected by the viscosity used. In the future, a decision is needed as to the most suitable form for representing the diffusion in order to simulate accurately the flow in the atmosphere.

In conclusion, the test integration showed that:

(a) A system of primitive equations formulated by the box method could be time integrated over a global domain for 50 days without any sign of finite-difference computational trouble.

(b) The nine-level model of the atmosphere withstood an initial imbalance in the wind field, and a rather high-amplitude seiche of air between the poles and the equator was damped out.

(c) Baroclinic waves of wave number 5 to 7 developed in the model, the predicted patterns of the variables remained smooth, and the behavior of the disturbances was reasonable.

(d) The accuracy in estimation of the budgets of energy and absolute angular momentum was reaffirmed by the analysis of the test integration.

(e) The appropriate formulations of momentum diffusion seem to be required for the accurate simulation of the flow.

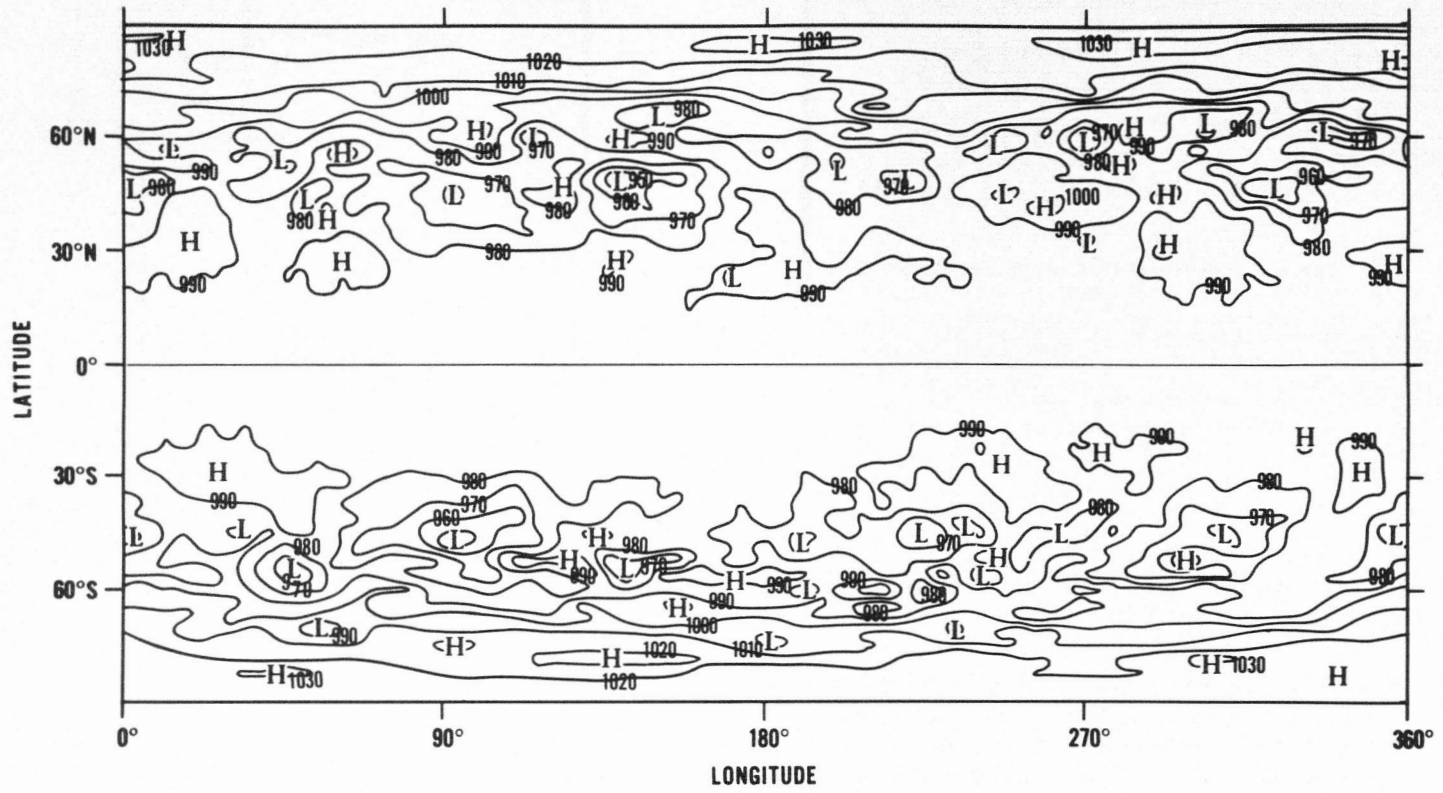

FIGURE 16.—Surface pressure map at 50 days for the run started from 40 days of the standard run but computed without horizontal viscosity. Contours are drawn every 10 mb.

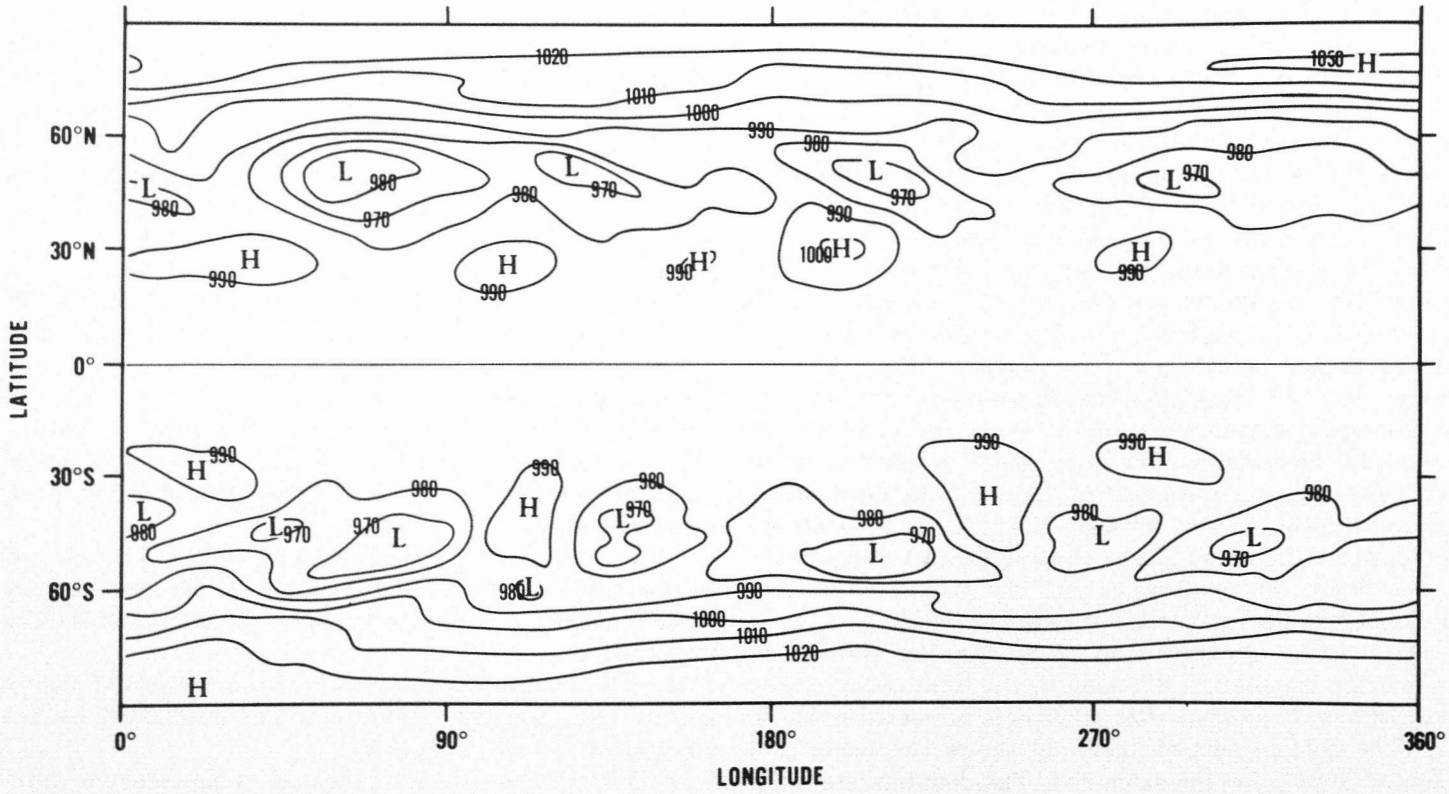

FIGURE 17.—Surface pressure map at 50 days for the run started from 40 days of the standard run but computed with horizontal diffusion in the form of non-linear viscosity. Contours are drawn every 10 mb.

Appendix 1.

FINITE-DIFFERENCE FORMS OF THE FRICTIONAL FORCE, ENERGY DISSIPATION, AND HEAT DIFFUSION

FRICTIONAL FORCE

The frictional force term F_λ in the equation (3.1) and F_θ in (3.2) represent the rate of change of P_*u and P_*v resulting from the diffusion of momentum. Let us define the following:

$\tau^{\lambda\lambda}$ westward diffusive flux of eastward momentum
$\tau^{\lambda\theta}$ southward diffusive flux of eastward momentum
$\tau^{\lambda z}$ downward diffusive flux of eastward momentum
$\tau^{\theta\lambda}$ westward diffusive flux of northward momentum
$\tau^{\theta\theta}$ southward diffusive flux of northward momentum
$\tau^{\theta z}$ downward diffusive flux of northward momentum

Then, F_λ and F_θ written in the λ, θ, z coordinate system and in the λ, θ, σ coordinate system, respectively, take the following forms:

$$F_\lambda=\frac{P_*}{\rho}\left[\frac{\partial\tau^{\lambda\lambda}}{a\partial\lambda}+\frac{\partial\tau^{\lambda\theta}\cos^2\theta}{a\cos\theta\partial\theta}+\frac{\partial\tau^{\lambda z}}{\partial z}\right]=-\frac{\partial}{a\partial\lambda}\left(\tau^{\lambda\lambda}\frac{\partial\phi}{\partial\sigma}\right)$$
$$+\frac{\partial}{\partial\sigma}\left(\tau^{\lambda\lambda}\frac{\partial\phi}{a\partial\lambda}\right)+\frac{1}{\cos\theta}\left[-\frac{\partial}{a\partial\theta}\left(\tau^{\lambda\theta}\cos^2\theta\frac{\partial\phi}{\partial\sigma}\right)\right.$$
$$\left.+\frac{\partial}{\partial\sigma}\left(\tau^{\lambda\theta}\cos\theta\frac{\partial\phi}{a\partial\theta}\right)\right]-g\frac{\partial\tau^{\lambda z}}{\partial\sigma} \quad \text{(A1.1)}$$

$$F_\theta=\frac{P_*}{\rho}\left[\frac{\partial\tau^{\theta\lambda}}{a\partial\lambda}+\frac{\partial\tau^{\theta\theta}\cos\theta}{a\partial\theta}+\frac{\tan\theta}{a}\tau^{\lambda\lambda}+\frac{\partial\tau^{\theta z}}{\partial z}\right]$$
$$=-\frac{\partial}{a\partial\lambda}\left(\tau^{\theta\lambda}\frac{\partial\phi}{\partial\sigma}\right)+\frac{\partial}{\partial\sigma}\left(\tau^{\theta\lambda}\frac{\partial\phi}{a\partial\lambda}\right)-\frac{\partial}{a\partial\theta}\left(\tau^{\theta\theta}\cos\theta\frac{\partial\phi}{\partial\sigma}\right)$$
$$+\frac{\partial}{\partial\sigma}\left(\tau^{\theta\theta}\frac{\partial\phi}{a\partial\theta}\right)-\frac{\tan\theta}{a}\tau^{\lambda\lambda}\frac{\partial\phi}{\partial\sigma}-g\frac{\partial\tau^{\theta z}}{\partial\sigma} \quad \text{(A1.2)}$$

The boundary conditions are

$$\tau^{\lambda\lambda}=\tau^{\lambda\theta}=\tau^{\lambda z}=\tau^{\theta\lambda}=\tau^{\theta\theta}=\tau^{\theta z}=0 \text{ at } \sigma=0 \quad \text{(A1.3)}$$

$$\left.\begin{aligned}\left(\tau^{\lambda z}-\tau^{\lambda\lambda}\frac{\partial z}{a\partial\lambda}-\tau^{\lambda\theta}\frac{\partial z}{a\partial\theta}\right)_{\sigma=1}&=\tau^{\lambda}_{ES}\\ \left(\tau^{\theta z}-\tau^{\theta\lambda}\frac{\partial z}{a\partial\lambda}-\tau^{\theta\theta}\frac{\partial z}{a\partial\theta}\right)_{\sigma=1}&=\tau^{\theta}_{ES}\end{aligned}\right\} \quad \text{(A1.4)}$$

The quantity τ^{λ}_{ES} is a diffusive transfer of eastward momentum from the atmosphere to the earth across the surface $\sigma=1$, flat or sloping, and τ^{θ}_{ES} is the corresponding term for northward momentum.

The horizontal diffusive flux of momentum will be written in the form of the so-called non-linear viscosity as well as in a linear form.

According to Smagorinsky [7], the non-linear viscosity can be formulated by (A1.5) and (A1.7):

$$\tau^{\lambda\lambda}=-\tau^{\theta\theta}=\rho\Gamma D_T$$
$$=-P_*\frac{\partial\sigma}{\partial\phi}\Gamma D_T \qquad \text{(in } \lambda, \theta, \sigma \text{ coordinates)} \quad \text{(A1.5)}$$

where the tension rate of strain D_T, is given by

$$D_T=\frac{\partial u}{a\partial\lambda}-\frac{\cos\theta}{a}\frac{\partial}{\partial\theta}\left(\frac{v}{\cos\theta}\right) \qquad \text{(in } \lambda, \theta, z \text{ coordinates)}$$
$$=\left(\frac{\partial\sigma}{\partial\phi}\right)\left[\frac{\partial\phi}{\partial\sigma}\frac{\partial u}{a\partial\lambda}-\frac{\partial\phi}{a\partial\lambda}\frac{\partial u}{\partial\sigma}-\frac{\partial\phi}{\partial\sigma}\frac{\tan\theta}{a}v-\frac{\partial\phi}{\partial\sigma}\frac{\partial v}{a\partial\theta}+\frac{\partial\phi}{a\partial\theta}\frac{\partial v}{\partial\sigma}\right]$$
$$\text{(in } \lambda, \theta, \sigma \text{ coordinates)} \quad \text{(A1.6)}$$

and

$$\tau^{\lambda\theta}=\tau^{\theta\lambda}=\rho\Gamma D_S$$
$$=-P_*\frac{\partial\sigma}{\partial\phi}\Gamma D_S \qquad \text{(in } \lambda, \theta, \sigma \text{ coordinates)} \quad \text{(A1.7)}$$

where D_S is the shearing rate of strain given below in the two coordinate systems

$$D_S=\frac{\partial v}{a\partial\lambda}+\frac{\cos\theta}{a}\frac{\partial}{\partial\theta}\left(\frac{u}{\cos\theta}\right)$$
$$=\left(\frac{\partial\sigma}{\partial\phi}\right)\left\{\frac{\partial\phi}{\partial\sigma}\frac{\partial v}{a\partial\lambda}-\frac{\partial\phi}{a\partial\lambda}\frac{\partial v}{\partial\sigma}\right.$$
$$\left.+\cos\theta\left[\frac{\partial\phi}{\partial\sigma}\frac{\partial}{a\partial\theta}\left(\frac{u}{\cos\theta}\right)-\frac{\partial\phi}{a\partial\theta}\frac{\partial}{\partial\sigma}\left(\frac{u}{\cos\theta}\right)\right]\right\} \quad \text{(A1.8)}$$

In (A1.5) and (A1.7), Γ is defined by

$$\Gamma=(\kappa_{\text{eff}})^{-2}|D| \quad \text{(A1.9)}$$

where κ_{eff} is the effective wave number having the dimensions of (length)$^{-1}$, and $|D|$ is pure deformation, i.e., $|D|=[D_T^2+D_S^2]^{1/2}$ which has the dimension (time)$^{-1}$.

In the version of linear viscosity, the horizontal stresses written in the λ, θ, z coordinate system are:

$$\tau^{\lambda\lambda}=\rho K_H\left(\frac{\partial u}{a\partial\lambda}-\frac{\tan\theta}{a}v\right)$$
$$\tau^{\lambda\theta}=\rho K_H\cos\theta\frac{\partial}{a\partial\theta}\left(\frac{u}{\cos\theta}\right)$$
$$\tau^{\theta\lambda}=\rho K_H\frac{\partial v}{a\partial\lambda}$$
$$\tau^{\theta\theta}=\rho K_H\frac{\partial v}{a\partial\theta}$$

In the above definition, K_H is the horizontal eddy viscosity coefficient having the dimensions of (length)$^2\cdot$(time)$^{-1}$.

On the other hand, the vertical diffusive flux of momentum is usually defined as follows:

$$\tau^{\lambda z}=\rho K_V\frac{\partial u}{\partial z}=-g\frac{P_*}{R^2}\frac{\sigma^2}{T^2}K_V\frac{\partial u}{\partial\sigma} \tag{A1.10}$$

$$\tau^{\theta z}=\rho K_V\frac{\partial v}{\partial z}=-g\frac{P_*}{R^2}\frac{\sigma^2}{T^2}K_V\frac{\partial v}{\partial\sigma} \tag{A1.11}$$

where K_V is the vertical eddy viscosity coefficient with the dimensions (length)$^2\cdot$(time)$^{-1}$.

In formulating the finite-difference schemes of the frictional force, we need to determine what kind of stress is acting at an interface between the key box and an adjacent box l. Refer to figure A1 for definitions. Westward diffusive fluxes of momentum, denoted by $\tau^{\lambda\lambda}_{0lk}$ and $\tau^{\theta\lambda}_{0lk}$ in the figure, are defined at the 0–l interfaces on the east and the west sides of the box; southward fluxes, $\tau^{\lambda\theta}_{0lk}$ and $\tau^{\theta\theta}_{0lk}$, are at the north and the south interfaces; and downward fluxes, $\tau^{\lambda z}_{0k-1/2}$ and $\tau^{\theta z}_{0k-1/2}$, are at the bottom and the top of the box.

The finite-difference forms corresponding to (A1.1) and (A1.2) in the λ, θ, σ coordinate system can be obtained by using the following rules. Let X be a component of the Reynolds stress tensor. Then, the quantities on the left-hand sides of the formulas written below are expressed by the forms on the right-hand sides.

$$\frac{\partial}{\alpha\partial\lambda}\left(X\frac{\partial\phi}{\partial\sigma}\right)=\left(\sum_E-\sum_W\right)\{XW\}$$

$$\frac{\partial}{\alpha\partial\theta}\left(X\cos\theta\frac{\partial\phi}{\partial\sigma}\right)=\left(\sum_N-\sum_S\right)\{XW\} \tag{A1.12}$$

where

$$\{XW\}\equiv X_{0lk}\frac{(\delta_k\phi)_{0l}}{\delta_k\sigma}w_l$$

$$\frac{\partial}{\partial\sigma}\left(X\frac{\partial\phi}{\alpha\partial\lambda}\right)=\frac{1}{2}\frac{1}{\delta_k\sigma}\left[\sum_E\{XPW\}-\sum_W\{XPW\}\right]$$

$$\frac{\partial}{\partial\sigma}\left(X\frac{\partial\phi}{a\partial\theta}\right)=\frac{1}{2}\frac{1}{\delta_k\sigma}\left[\sum_N\{XPW\}-\sum_S\{XPW\}\right] \tag{A1.13}$$

where

$$\{XPW\}\equiv\left[\left(\frac{X_{0lk+1}+X_{0lk}}{2}\right)(\phi_l-\phi_0)_{k+1/2}-\left(\frac{X_{0lk}+X_{0lk-1}}{2}\right)(\phi_l-\phi_0)_{k-1/2}\right]w_l$$

$$\frac{\tan\theta}{a}X\frac{\partial\phi}{\partial\sigma}=\frac{1}{2}\frac{\tan\theta_0}{a}\left[\sum_E\{XW\}/(w_E)_0+\sum_W\{XW\}/(w_W)_0\right] \tag{A1.14}$$

$$\frac{\partial X}{\partial\sigma}=\frac{1}{\delta_k\sigma}(X_{0k+1/2}-X_{0k-1/2}) \tag{A1.15}$$

In the above formulas,

$$\frac{(\delta_k\phi)_{0l}}{\delta_k\sigma}=\frac{1}{\delta_k\sigma}\left(\frac{\phi_{lk+1/2}+\phi_{0k+1/2}}{2}-\frac{\phi_{lk-1/2}+\phi_{0k-1/2}}{2}\right)$$

If X in (A1.12) and (A1.13) is replaced by $X\cos\theta$, X_{0lk} on the right-hand side should be $X_{0lk}\cos\theta_N$ or $X_{0lk}\cos\theta_S$. The divisor $\cos\theta$ in (A1.1) should be $\cos\theta_0$ in the finite-difference formulation. The conditions which are consistent with (A1.3) and (A1.4) can be obtained by assuming that

$$X_{0l0}=-X_{0l1}$$

$$X_{0l\frac{1}{2}}=0$$

and

$$X_{0lK+1}=-X_{0lK}$$

$$X_{0K+\frac{1}{2}}=(X_{ES})_0$$

In the finite-difference forms corresponding to (A1.5) and (A1.7) $P_*\frac{\partial\sigma}{\partial\phi}$ takes the form

$$\frac{P_{*0}+P_{*l}}{2}\cdot\left[\frac{\delta_k\sigma}{(\delta_k\phi)_{0l}}\right]$$

The deformation at the interface of the boxes, i.e., (A1.6) and (A1.8), can be estimated by applying the following rules:

$\frac{\partial\phi}{\partial\sigma}\cdot\frac{\partial A}{\alpha\partial\lambda}$ at the east interface or $\frac{\partial\phi}{\partial\sigma}\cdot\frac{\partial A}{a\partial\theta}$ at the north interface

$$=\frac{(\delta_k\phi)_{0l}}{\delta_k\sigma}(A_l-A_0)\cdot\frac{(w_{E\text{ or }N})_0+(w_{W\text{ or }S})_l}{2} \tag{A1.16}$$

where A is a given variable.

$\frac{\partial\phi}{\alpha\partial\lambda}\cdot\frac{\partial A}{\partial\sigma}$ at the east interface or $\frac{\partial\phi}{a\partial\theta}\cdot\frac{\partial A}{\partial\sigma}$ at the north interface

$$=\frac{1}{2}\left\{(\phi_l-\phi_0)_{k+1/2}\left(\frac{A_{0k+1}+A_{lk+1}}{2}-\frac{A_{0k}+A_{lk}}{2}\right)+(\phi_l-\phi_0)_{k-1/2}\left(\frac{A_{0k}+A_{lk}}{2}-\frac{A_{0k-1}+A_{lk-1}}{2}\right)\right\}\times\frac{1}{\delta_k\sigma}\left[\frac{(w_{E\text{ or }N})_0+(w_{W\text{ or }S})_l}{2}\right] \tag{A1.17}$$

$\frac{\partial\phi}{\partial\sigma}\cdot\frac{\tan\theta}{a}v$ at the east interface

$$=\frac{(\delta_k\phi)_{0l}}{\delta_k\sigma}\cdot\frac{1}{2a}\left[\frac{v_0\tan\theta_0}{(w_E)_0}+\frac{v_l\tan\theta_l}{(w_W)_l}\right]\cdot\frac{(w_E)_0+(w_W)_l}{2} \tag{A1.18}$$

When A in (A1.16) and (A1.17) is $u/\cos\theta$, A_0 should be estimated by $u_0/\cos\theta_0$. The multiplying factor $\cos\theta$ in (A1.8) should be $\cos\theta_N$ or $\cos\theta_S$ in the corresponding

finite-difference form. The values corresponding to (A1.16), (A1.17), and (A1.18) at the west or south interfaces are obtained by exchanging the subscripts 0 and l in the above formulas. In the finite-difference formulation of deformation, the zonal variation of a quantity at a north or south interface and the meridional variation at an east or west interface are taken to be zero, and the factor $(v/a)\tan\theta$ in tension is taken into consideration only at the east and west interfaces. Finally, the assumptions $A_{00}=A_{01}$, $A_{0K+1}=A_{0K}$ should also be used. The coefficient Γ in (A1.5) and (A1.7) is estimated at each lateral interface by $(\kappa_{\text{eff}})^{-2}|D|$, where

$$(\kappa_{\text{eff}})_l^{-2}=2k_0^2(A_l/\delta_k\sigma)^2 \quad \text{and} \quad |D|=[(D_T)^2+(D_S)^2]^{1/2}$$

The k_0 in the above is a non-dimensional parameter of order unity.

The form of the vertical stress corresponding to (A1.10) is shown below as an example:

$$\tau^{\lambda z}_{0k+\frac{1}{2}}=-g\frac{P_{*0}}{R^2}\cdot\frac{\sigma^2_{k+\frac{1}{2}}}{T^2_{k+\frac{1}{2}}}\cdot K_{V_{k+\frac{1}{2}}}\cdot\frac{u_{0k+1}-u_{0k}}{\sigma_{k+1}-\sigma_k}$$

where

$$\sigma_k=\tfrac{1}{2}(\sigma_{k+\frac{1}{2}}+\sigma_{k-\frac{1}{2}})$$
$$T_{k+\frac{1}{2}}=\tfrac{1}{2}(T_{k+1}+T_k) \qquad \text{(A1.19)}$$

The above equation does not apply when $k=0$ and K.

ENERGY DISSIPATION

The dissipation of kinetic energy is derived here in λ, θ, σ coordinates. The inner product of horizontal wind and the frictional force can be divided into three parts; namely,

$$uF_\lambda+vF_\theta=(\text{WKLT})+(\text{WKSG})+(\text{DIS}) \qquad \text{(A1.20)}$$

where (WKLT) represents the work done by wind stress through the lateral boundary; (WKSG), the work done through sigma surfaces; and (DIS), the internal dissipation of kinetic energy. Furthermore, both uF_λ and vF_θ can be separated in the same way,

$$uF_\lambda=(\text{WKLT})_1+(\text{WKSG})_1+(\text{DIS})_1$$
$$vF_\theta=(\text{WKLT})_2+(\text{WKSG})_2+(\text{DIS})_2$$

These six components are written as follows:

$$(\text{WKLT})_1=-\frac{\partial}{\alpha\partial\lambda}\left(\tau^{\lambda\lambda}\frac{\partial\phi}{\partial\sigma}u\right)-\frac{\partial}{\alpha\partial\theta}\left(\tau^{\lambda\theta}\cos^2\theta\frac{\partial\phi}{\partial\sigma}\frac{u}{\cos\theta}\right)$$

$$(\text{WKLT})_2=-\frac{\partial}{\alpha\partial\lambda}\left(\tau^{\theta\lambda}\frac{\partial\phi}{\partial\sigma}v\right)-\frac{\partial}{\alpha\partial\theta}\left(\tau^{\theta\theta}\cos\theta\frac{\partial\phi}{\partial\sigma}v\right)$$

$$(\text{WKSG})_1=\frac{\partial}{\partial\sigma}\left(\tau^{\lambda\lambda}u\frac{\partial\phi}{\alpha\partial\lambda}+\tau^{\lambda\theta}u\frac{\partial\phi}{a\partial\theta}-g\tau^{\lambda z}u\right)$$

$$(\text{WKSG})_2=\frac{\partial}{\partial\sigma}\left(\tau^{\theta\lambda}v\frac{\partial\phi}{\alpha\partial\lambda}+\tau^{\theta\theta}v\frac{\partial\phi}{a\partial\theta}-g\tau^{\theta z}v\right)$$

$$(\text{DIS})_1=\tau^{\lambda\lambda}\left(\frac{\partial\phi}{\partial\sigma}\frac{\partial u}{\alpha\partial\lambda}-\frac{\partial\phi}{\alpha\partial\lambda}\frac{\partial u}{\partial\sigma}\right)$$
$$+\tau^{\lambda\theta}\cos\theta\left[\frac{\partial\phi}{\partial\sigma}\frac{\partial}{a\partial\theta}\left(\frac{u}{\cos\theta}\right)-\frac{\partial\phi}{a\partial\theta}\frac{\partial}{\partial\sigma}\left(\frac{u}{\cos\theta}\right)\right]+\tau^{\lambda z}g\frac{\partial u}{\partial\sigma}$$

$$(\text{DIS})_2=\tau^{\theta\lambda}\left(\frac{\partial\phi}{\partial\sigma}\frac{\partial v}{\alpha\partial\lambda}-\frac{\partial\phi}{\alpha\partial\lambda}\frac{\partial v}{\partial\sigma}\right)$$
$$+\tau^{\theta\theta}\left(\frac{\partial\phi}{\partial\sigma}\frac{\partial v}{a\partial\theta}-\frac{\partial\phi}{a\partial\theta}\frac{\partial v}{\partial\sigma}\right)-\tau^{\lambda\lambda}\left(\frac{\partial\phi}{\partial\sigma}\frac{\tan\theta}{a}v\right)+\tau^{\theta z}g\frac{\partial v}{\partial\sigma}$$

Vertical integration of (WKSG), by means of (A1.3) and (A1.4), yields the dissipation of kinetic energy at the ground surface by the work done against the surface stress:

$$\int_0^1(\text{WKSG})\frac{d\sigma}{g}=-(\tau^\lambda_{ES}\cdot u_{\sigma=1}+\tau^\theta_{ES}\cdot v_{\sigma=1}) \qquad \text{(A1.21)}$$

On the other hand, the global area integration of (WKLT) vanishes.

$$\iint_{\Delta S}(\text{WKLT})dS=0 \qquad \text{(A1.22)}$$

The internal dissipation in the case of non-linear viscosity becomes

$$(\text{DIS})=-P_*\Gamma(D_T^2+D_S^2)-P_*K_V\left(\frac{g\sigma}{RT}\right)^2\left[\left(\frac{\partial u}{\partial\sigma}\right)^2+\left(\frac{\partial v}{\partial\sigma}\right)^2\right] \qquad \text{(A1.23)}$$

Using the frictional forces expressed according to the previously mentioned rules, we can define the finite-difference forms of (WKSG), (DIS), and (WKLT) so that the following conditions which correspond to (A1.20), (A1.21), and (A1.22), respectively, are satisfied:

$$u_0(F_\lambda)_0+v_0(F_\theta)_0=(\text{WKLT})_0+(\text{WKSG})_0+(\text{DIS})_0$$

$$\sum_{k=1}^{K}(\text{WKSG})_{ijk}\frac{\delta_k\sigma}{g}=-[(\tau^\lambda_{ES})_0u_{0K+1/2}+(\tau^\theta_{ES})_0v_{0K+1/2}]$$

$$\sum_i\sum_j(\text{WKLT})_{ijk}\Delta S_{ij}=0$$

The internal dissipation takes the form corresponding to (A1.23)

$$(\mathrm{DIS})_0=-\frac{1}{2}\Bigg[\sum_E \frac{P_{*0}+P_{*l}}{2}\,\Gamma_{0lk}|D|^2_{0lk}\,\frac{2}{(w_E)_0+(w_W)_l}\,w_l$$

$$+\sum_W \frac{P_{*0}+P_{*l}}{2}\,\Gamma_{0lk}|D|^2_{0lk}\,\frac{2}{(w_W)_0+(w_E)_l}\,w_l\Bigg]$$

$$-\frac{1}{2}\Bigg[\sum_N \frac{P_{*0}+P_{*l}}{2}\,\Gamma_{0lk}|D|^2_{0lk}\,\frac{2}{(w_N)_0+(w_S)_l}\,w_l$$

$$+\sum_S \frac{P_{*0}+P_{*l}}{2}\,\Gamma_{0lk}|D|^2_{0lk}\,\frac{2}{(w_S)_0+(w_N)_l}\,w_l\Bigg]$$

$$-\frac{1}{2}\,[(A)+(B)] \qquad \text{(A1.24)}$$

where

$$(A)=\begin{cases} P_{*0}\left(\dfrac{g}{R}\right)^2 K_{V_{k+\frac{1}{2}}}\left(\dfrac{\sigma_{k+\frac{1}{2}}}{T_{k+\frac{1}{2}}}\right)^2\{(u_{0k+1}-u_{0k})^2 \\ \qquad +(v_{0k+1}-v_{0k})^2\}\,\dfrac{1}{\sigma_{k+1}-\sigma_k}\,\dfrac{1}{\delta_k\sigma} \text{ for } k\neq K \\ -g\,\dfrac{2}{\delta_k\sigma}\,\{(\tau^{\lambda}_{ES})_0(u_{0k+\frac{1}{2}}-u_{0k}) \\ \qquad +(\tau^{\theta}_{ES})_0(v_{0k+\frac{1}{2}}-v_{0k})\} \text{ for } k=K \end{cases}$$

$$(B)=\begin{cases} 0 \text{ for } k=1 \\ P_{*0}\left(\dfrac{g}{R}\right)^2 K_{V_{k-\frac{1}{2}}}\left(\dfrac{\sigma_{k-\frac{1}{2}}}{T_{k-\frac{1}{2}}}\right)^2\{(u_{0k}-u_{0k-1})^2 \\ \qquad +(v_{0k}-v_{0k-1})^2\}\,\dfrac{1}{\sigma_k-\sigma_{k-1}}\,\dfrac{1}{\delta_k\sigma} \text{ for } k\neq 1 \end{cases}$$

It would be desirable that the relation between the assumed surface wind $\mathbf{V}_{0K+\frac{1}{2}}$ and $\mathbf{V}_{0K}$ is such that the value (A) in the above formula becomes positive when $k=K$.

If we assume that the air-earth exchange of momentum along a slope is the same as it is over a horizontal plane, $(\tau^{\lambda}_{ES})_0$ and $(\tau^{\theta}_{ES})_0$ may be estimated, given the drag coefficient C_D, by

$$(\tau^{\lambda}_{ES})_0=(\rho C_D|\mathbf{V}|u)_{0K+\frac{1}{2}}\cdot s_0$$

$$(\tau^{\theta}_{ES})_0=(\rho C_D|\mathbf{V}|v)_{0K+\frac{1}{2}}\cdot s_0$$

where s_0 is an area factor; $s_0=\{1+[G_\lambda(z_*)]^2+[G_\theta(z_*)]^2\}$, in which z_* denotes the height of the ground surface.

HEAT DIFFUSION

In the following let us define γ^λ as the westward diffusive flux of heat; γ^θ the southward diffusive flux of heat; and γ^z the downward diffusive flux of heat. The rate of change of P_*T due to heat diffusion, i.e., F_T in equation (3.3), is given by

$$F_T=\frac{P_*}{\rho}\left[\frac{\partial\gamma^\lambda}{a\partial\lambda}+\frac{\partial\gamma^\theta\cos\theta}{a\partial\theta}+\frac{\partial\gamma^z}{\partial z}\right] \qquad \text{(in } \lambda,\ \theta,\ z \text{ coordinates)}$$

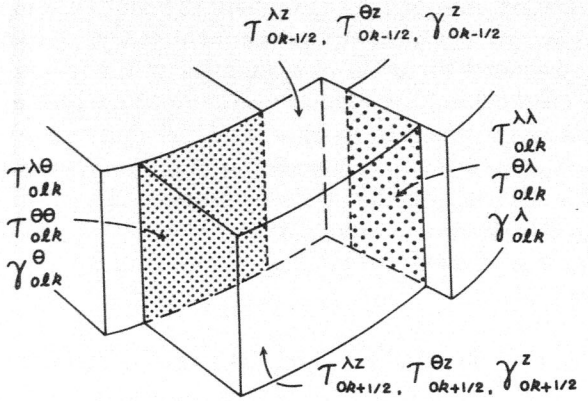

FIGURE A1.—Diagram of the locations of the westward diffusive fluxes of momentum, $\tau^{\lambda\lambda}_{0lk}$ and $\tau^{\theta\lambda}_{0lk}$, and westward diffusive flux of heat, γ^{λ}_{0lk}, at an east interface of the key box with an adjacent box; the southward diffusive fluxes of momentum, $\tau^{\lambda\theta}_{0lk}$ and $\tau^{\theta\theta}_{0lk}$, and southward diffusive flux of heat, γ^{θ}_{0lk}, at a north interface of the key box with another contiguous box; and the downward diffusive fluxes, $\tau^{\lambda z}_{0k+\frac{1}{2}}$ and $\tau^{\theta z}_{0k+\frac{1}{2}}$, of momentum and of heat, $\gamma^{z}_{0k+\frac{1}{2}}$, at the bottom of the key box.

$$=-\frac{\partial}{\alpha\partial\lambda}\left(\gamma^\lambda\frac{\partial\phi}{\partial\sigma}\right)+\frac{\partial}{\partial\sigma}\left(\gamma^\lambda\frac{\partial\phi}{\alpha\partial\lambda}\right)-\frac{\partial}{\alpha\partial\theta}\left(\gamma^\theta\cos\theta\,\frac{\partial\phi}{\partial\sigma}\right)$$

$$+\frac{\partial}{\partial\sigma}\left(\gamma^\theta\frac{\partial\phi}{a\partial\theta}\right)-g\,\frac{\partial\gamma^z}{\partial\sigma} \qquad \text{(in } \lambda,\ \theta,\ \sigma \text{ coordinates)} \qquad \text{(A1.25)}$$

The conditions at the upper and the lower boundaries are

$$\gamma^\lambda=\gamma^\theta=\gamma^z=0 \text{ at } \sigma=0 \qquad \text{(A1.26)}$$

$$\left(\gamma^z-\gamma^\lambda\frac{\partial z}{\alpha\partial\lambda}-\gamma^\theta\frac{\partial z}{a\partial\theta}\right)_{\sigma=1}=\gamma_{ES} \text{ at } \sigma=1 \qquad \text{(A1.27)}$$

The quantity γ_{ES} represents the diffusive transfer of heat to the earth across the surface $\sigma=1$.

With the horizontal and vertical eddy diffusion coefficients for heat denoted by A_H and A_V, both of which have the dimensions $(\text{length})^2\cdot(\text{time})^{-1}$, the heat diffusion fluxes are expressed in λ, θ, z and λ, θ, σ coordinates respectively:

$$\gamma^\lambda=\rho A_H\frac{\partial T}{\alpha\partial\lambda}$$

$$=-P_*\frac{\partial\sigma}{\partial\phi}A_H\frac{\partial\sigma}{\partial\phi}\left(\frac{\partial\phi}{\partial\sigma}\frac{\partial T}{\alpha\partial\lambda}-\frac{\partial\phi}{\alpha\partial\lambda}\frac{\partial T}{\partial\sigma}\right) \qquad \text{(A1.28)}$$

$$\gamma^\theta=\rho A_H\frac{\partial T}{a\partial\theta}$$

$$=-P_*\frac{\partial\sigma}{\partial\phi}A_H\frac{\partial\sigma}{\partial\phi}\left(\frac{\partial\phi}{\partial\sigma}\frac{\partial T}{a\partial\theta}-\frac{\partial\phi}{a\partial\theta}\frac{\partial T}{\partial\sigma}\right) \qquad \text{(A1.29)}$$

$$\gamma^z=\rho A_V\frac{\partial T}{\partial z}$$

$$=-g\frac{P_*}{R^2}\frac{\sigma^2}{T^2}A_V\frac{\partial T}{\partial\sigma} \qquad \text{(A1.30)}$$

As shown in figure A1, γ^λ, γ^θ, and γ^z are defined at the east and west interfaces, at the north and south interfaces, and at the bottom and top of the box, respectively. The finite-difference forms of heat diffusion fluxes and F_T can be formulated by using the same rules as those employed in the formulation of the frictional forces.

Appendix 2.

SPECIAL FINITE-DIFFERENCE FORMS FOR THE TWO POLAR BOXES

If, as is the case when using system 1 in Kurihara's paper ([2], p. 401), a grid point is situated on the north or south pole, special finite-difference forms of the equations are needed. However, the occurrence of a polar box can be avoided, for example, by adopting the grid system 3 in [2].

Assume that the north polar box is surrounded by four boxes as shown in figure A2. In this case, the box is bounded by only three surfaces, i.e., $\theta=\theta_S=\frac{\pi}{2}-\frac{\Delta\theta}{2}$, $\sigma=\sigma_{k+1/2}$, and $\sigma=\sigma_{k-1/2}$. The horizontal cross-section and volume of the box are

$$\Delta S=2\pi a^2(1-\sin\theta_S)$$
$$\Delta V=\Delta S\cdot\delta\sigma \qquad \text{(A2.1)}$$

Since the four lateral interfaces have the same area, their weights computed by (2.3) are $w_1=w_2=w_3=w_4=w$.

The integrated mean of the wind in the north polar box is defined by U and V (see fig. A2). If the wind at the polar box is observed from the surrounding boxes in the figure, U and V are taken as

$U=u,\quad V=v$ by the box $l=1$,
$U=-v,\quad V=u$ by the box $l=2$,
$U=-u,\quad V=-v$ by the box $l=3$,
$U=v,\quad V=-u$ by the box $l=4$.

These relations must be used in obtaining the finite-difference forms for the surrounding boxes. Figure A2 can be made to represent the south polar box by exchanging the indices for boxes one and three. However, the conversions between small and capital u and v are changed accordingly.

The finite-difference forms of the system of equations for the polar boxes including the prognostic equations for P_*U and P_*V are obtained in the same manner as derived in Section 3 for the other boxes. In the derivation, due regard is given to the above wind field definitions. For example, the rate of change of P_{*0} at the north pole is given by

$$\frac{\partial}{\partial t}P_{*0}=\left[\frac{P_{*1}+P_{*0}}{2}\cdot\frac{v_1+V}{2}+\frac{P_{*2}+P_{*0}}{2}\cdot\frac{v_2-U}{2}+\frac{P_{*3}+P_{*0}}{2}\cdot\frac{v_3-V}{2}+\frac{P_{*4}+P_{*0}}{2}\cdot\frac{v_4+U}{2}\right]_k w-\frac{P_{*0}}{\delta_k\sigma}(\bar{\omega}_{k+1/2}-\omega_{k-1/2}) \qquad \text{(A2.2)}$$

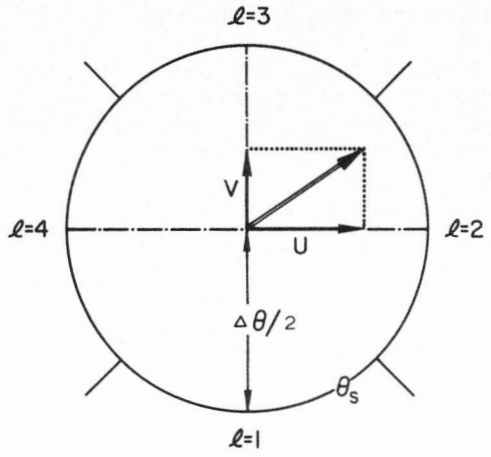

FIGURE A2.—Diagram of the U and V wind components in the north polar box surrounded by boxes $l=1$ through 4. Observed from box 2 the U-component appears as a northerly wind ($v<0$) and the V-component, a west wind ($u>0$).

If the thermal equation and the equation of kinetic energy are derived, it is seen that the horizontal inflow of energy into the polar boxes is the same as the outflow across the poleward boundaries of the surrounding boxes.

The finite-difference forms of the frictional forces, energy dissipation, and the effect of heat diffusion in the polar boxes can also be obtained by using $\tau^{\lambda\theta}$, $\tau^{\theta\theta}$, and γ^θ which are defined at the poleward sides of the surrounding boxes.

ACKNOWLEDGMENTS

We wish to thank Dr. K. Bryan for many helpful discussions which contributed greatly to this work. We appreciate the encouragement given by Drs. J. Smagorinsky and S. Manabe of the Geophysical Fluid Dynamics Laboratory, ESSA, and Dr. K. Takahashi, of the Meteorological Research Institute. We were greatly assisted by suggestions of a number of persons who read our manuscript, notably Drs. K. Miyakoda and G. Williams of GFDL. Our thanks are due to Mrs. C. Bunce of GFDL for typing the manuscript and to Mrs. H. Shinoda of the Meteorological Research Institute, and Mr. C. Gardner of ESSA for preparing the figures. We are indebted to Mrs. W. M. Carlton for programing the model equations on both the Control Data 6600 and UNIVAC 1108 computers, and to Mr. H. H. Engelbrecht and his staff of GFDL operators for running the program on the two machines.

REFERENCES

1. K. Bryan, "A Scheme for Numerical Integration of the Equations of Motion on an Irregular Grid Free of Nonlinear Instability," *Monthly Weather Review*, vol. 94, No. 1, Jan. 1966, pp. 39–40.
2. Y. Kurihara, "Numerical Integration of the Primitive Equations on a Spherical Grid," *Monthly Weather Review*, vol. 93, No. 7, July 1965, pp. 399–415.
3. F. G. Shuman, "Numerical Experiments with the Primitive Equations," *Proceedings of the International Symposium on Numerical Weather Prediction, Tokyo, 1960*, Meteorological Society of Japan, 1962, pp. 85–107.

269-089 O - 67 - 5

4. J. Smagorinsky, S. Manabe, and J. L. Holloway, Jr., "Numerical Results from a Nine-Level General Circulation Model of the Atmosphere," *Monthly Weather Review*, vol. 93, No. 12, Dec. 1965, pp. 727–768.
5. L. H. Underhill and L. M. Russell, "The Linear Transport Equation in One and Two Dimensions," *Numerical Solution of Ordinary and Partial Differential Equations*, edited by L. Fox, Pergamon Press, 1962, pp. 398–422.
6. W. F. Noh, Section IV of "CEL: A Time-Dependent Two-Space-Dimensional Coupled Eulerian-Lagrange Code," *Methods in Computational Physics*, vol. 3, edited by B. Alder, S. Fernbach, and M. Rotenberg, Academic Press, 1964, pp. 130–136.
7. J. Smagorinsky, "General Circulation Experiments with the Primitive Equations: I. The Basic Experiment," *Monthly Weather Review*, vol. 91, No. 3, Mar. 1963, pp. 99–164.

[*Received March 1, 1967; revised May 26, 1967*]